

**Hypoxia-induced epigenetic modifications are associated with cardiac tissue fibrosis and the development of a myofibroblast-like phenotype**

**Chris J. Watson<sup>1,2,\*</sup>, Patrick Collier<sup>1</sup>, Isaac Tea<sup>1</sup>, Roisin Neary<sup>1</sup>, Jenny A. Watson<sup>1</sup>, Claire Robinson<sup>1</sup>, Dermot Phelan<sup>1</sup>, Mark T. Ledwidge<sup>2</sup>, Kenneth M. McDonald<sup>2</sup>, Amanda McCann<sup>1</sup>, Osama Sharaf<sup>1</sup>, John A. Baugh<sup>1</sup>**

<sup>1</sup>School of Medicine & Medical Science, UCD Conway Institute, University College Dublin, Dublin, Belfield, Dublin 4, Ireland

<sup>2</sup>Chronic Cardiovascular Disease Management Unit, St Vincent's Healthcare Group/St Michael's Hospital, Co. Dublin, Ireland

\*Correspondence to: Chris Watson, PhD, School of Medicine & Medical Science, UCD Conway Institute, University College Dublin, Belfield, Dublin 4, Ireland. E-mail [chris.watson@ucd.ie](mailto:chris.watson@ucd.ie); Tel. +35317166729; Fax +35317166701.

## Abstract

Ischemia caused by coronary artery disease and myocardial infarction leads to aberrant ventricular remodeling and cardiac fibrosis. This occurs partly through accumulation of gene expression changes in resident fibroblasts, resulting in an overactive fibrotic phenotype. Long-term adaptation to a hypoxic insult is likely to require significant modification of chromatin structure in order to maintain the fibrotic phenotype. Epigenetic changes may play an important role in modulating hypoxia-induced fibrosis within the heart.

Therefore, the aim of the study was to investigate the potential pro-fibrotic impact of hypoxia on cardiac fibroblasts, and determine whether alterations in DNA methylation could play a role in this process.

This study found that within human cardiac tissue, the degree of hypoxia was associated with increased expression of collagen 1 and alpha smooth muscle actin (ASMA). In addition, human cardiac fibroblast cells exposed to prolonged 1% hypoxia resulted in a pro-fibrotic state. These hypoxia-induced pro-fibrotic changes were associated with global DNA hypermethylation and increased expression of the DNA methyltransferase (DNMT) enzymes DNMT1 and DNMT3B. Expression of these methylating enzymes was shown to be regulated by hypoxia-inducible factor (HIF)-1 $\alpha$ . Using siRNA to block DNMT3B expression significantly reduced collagen 1 and ASMA expression. In addition, application of the DNMT inhibitor 5-aza-2'-deoxycytidine suppressed the pro-fibrotic effects of TGF $\beta$ . Epigenetic modifications and changes in the epigenetic machinery identified in cardiac fibroblasts during prolonged hypoxia may contribute to the pro-fibrotic nature of the ischemic milieu. Targeting up-regulated expression of DNMTs in ischemic heart disease may prove to be a valuable therapeutic approach.

## Introduction

Cardiac fibrosis is a disease signified by a pathological increase in extracellular matrix (ECM) proteins that can result in structural remodeling of the heart (1). This process can occur as a normal physiological response to tissue injury where the heart responds to repair and preserve structure and function of the organ (2). As such, there is controlled deposition of ECM proteins, particularly collagen, with a regulatory element provided by ECM modifying enzymes, including the matrix metalloproteinases (MMPs). However, maladaptation of this wound repair process, either by persistent chronic injury or an inability to regulate the response, can result in a pathological reactive fibrosis which is detrimental to the functionality of the organ. Pathological cardiac fibrosis can develop from a number of stimuli including, ischemia, inflammation, pressure overload (observed in hypertensive heart disease and aortic stenosis), and volume overload (for example, mitral or aortic regurgitation) (2). A common feature of all these stimuli is tissue hypoxia, either directly occurring due to defects in oxygen supply or indirectly, due to increases in oxygen consumption by infiltrating inflammatory cells and activated resident cells. Prolonged local tissue hypoxia can lead to aberrant ventricular remodeling and cardiac fibrosis (3-5). One mechanism that is believed to contribute to this process is the accumulation of gene expression changes within the interstitium, resulting in an overactive fibrotic phenotype (6). Long term adaptation to this hypoxic insult is likely to require significant modification of chromatin structure in order to maintain the fibrotic phenotype. In this regard, we propose that epigenetic modifications, such as DNA methylation, play an important role in dictating cellular responses to chronic hypoxia and the progression of cardiac fibrosis.

DNA methylation is an epigenetic modification which involves the addition of methyl groups to cytosine residues already incorporated into DNA sequences, forming 5-methylcytosine (5MeC). This can either physically prevent transcription factor binding or reduce access to gene regulatory regions through local chromatin condensation, with both processes resulting in gene repression. DNA methylation is regulated by a family of DNA methyltransferase (DNMT) enzymes. DNMT1 preferentially methylates hemi-methylated DNA and is required to maintain the methylation pattern of the genome in daughter cells during cell division. DNMT3A and DNMT3B are *de novo* methylating

enzymes that are responsible for establishing the initial methylation patterns of the genome during development, whose expression re-emerges in disease states (7). Dysregulation of this process has been extensively studied in cancer, however its importance in fibrotic diseases is limited, particularly in the field of cardiac fibrosis (8-10). Therefore, the aim of this study was to investigate the pro-fibrotic impact of hypoxia, and whether alterations in DNA methylation could play a role in this process.

## Results

### **Myocardial tissue hypoxia is associated with an enhanced fibrotic gene expression profile.**

Following ethical approval and informed patient consent, human right atrial tissue samples were collected from the hearts of 26 patients undergoing elective cardiac surgery. RNA was extracted from this tissue and was used to look at the relationship between hypoxia and collagen production using quantitative real-time PCR. The degree of carbonic anhydrase IX (CAIX) expression was used as a validated surrogate marker for cardiac tissue hypoxia(11). Relative CAIX gene expression levels significantly correlated positively with ASMA ( $r=0.42$ ,  $p<0.05$ ), Figure 1A. A significant positive correlation between collagen 1 gene expression with CAIX was also detected ( $r=0.50$ ,  $p<0.01$ ), as highlighted in Figure 1B. Collagen 3 gene expression was not statistically associated with changes in CAIX expression, although a positive trend was observed ( $r=0.35$ ,  $p=0.08$ ).

### **Tissue hypoxia is associated with increased collagen deposition.**

The degree of collagen deposition within human atrial tissue samples was assessed using Masson's trichrome (MTC) staining. Examples of myocardial tissue stained with MTC can be observed in Figure 1D, with positive blue staining for collagen being evident, and myocytes staining red. This figure highlights examples of both interstitial and perivascular fibrosis. Two methods were used to analyze the collagen content within the MTC stained slides, namely, digital quantification of positive pixels (Figure 1E, an example where the positive pixel algorithm has been applied to a MTC stained slide generating a markup image detailing the positive blue pixels representing collagen) and blinded

manual scoring by a Pathologist (Figure 1F, examples of manual scoring images grading collagen deposition between 0-5).

The relationship between collagen deposition and hypoxia was assessed by dividing the MTC slides into two groups based on median CAIX gene expression levels. Results indicate that increased tissue hypoxia (higher CAIX expression) was associated with a significant increase in collagen ( $p < 0.05$ ). This was observed in both the automated digitally analyzed positive pixel quantification of collagen (Figure 1G) and the blinded manual scoring of MTC staining (Figure 1H).

### **Hypoxia induces a pro-fibrotic state in cardiac fibroblasts *in vitro*.**

These results indicate that the degree of hypoxia within myocardial tissue is associated with increased expression of the pro-fibrotic genes ASMA and collagen 1, as well as increased deposition of fibrillar collagen protein. As the likely source of the increased collagen within the myocardium is the cardiac fibroblast, we undertook *in vitro* hypoxia studies utilizing human primary cardiac fibroblast cells (HCF). HCF cells were cultured in either 21% oxygen or 1% oxygen for up to 8 days. Culturing cells in 1% oxygen stabilized nuclear HIF-1 $\alpha$  and increased the expression of CAIX, indicating that the cells were experiencing a hypoxic environment, Figure 2A and 2B, respectively. Under these conditions, an increase in cell proliferation was observed, another pathological feature of fibrosis, Figure 2C. Using quantitative real-time PCR, a significant increase in both ASMA and collagen 1 gene expression was detected at 4 and 8 days post hypoxia, compared with cells grown under normoxia, Figure 2D and 2E. Interestingly, the pro-fibrotic effects of TGF $\beta$ 1 treatment were enhanced in hypoxia. TGF $\beta$ 1 treatment of HCF significantly increased ASMA and collagen 1 gene expression, and this was further enhanced if the cells were exposed to 8 days hypoxia, Figure 2F and 2G, respectively.

### **Hypoxia causes DNA hypermethylation and increased DNA methyltransferase expression in cardiac fibroblasts.**

To determine whether the pro-fibrotic effects of hypoxia were associated with epigenetic changes within the HCF cells, DNA methylation studies were carried out. Global DNA methylation was

analyzed in cells exposed to either 21% oxygen, 1% oxygen for 4 days, or 1% oxygen for 8 days. Application of an antibody directed to methylated DNA (anti-5MeC) and quantification using flow cytometry revealed significant DNA hypermethylation in hypoxic cells ( $p < 0.001$ ), Figure 3A. Confirmation of specific nuclear staining was achieved using immunofluorescent microscopy, as highlighted in Figure 3B, with specific nuclear anti-5MeC positivity over a background of the blue nuclear counterstain DAPI. To investigate possible mechanisms of hypoxia induced DNA hypermethylation, the enzymes that catalyze this process were quantified, namely the DNA methyltransferases (DNMT). The gene expression levels of DNMT1, the enzyme primarily responsible for maintaining the methylation status of daughter cells during cell cycle, and the *de novo* methylating enzyme DNMT3B, were both significantly up-regulated as early as 24 hours following exposure to a 1% hypoxic environment ( $p < 0.001$ ), Figure 3C and 3E. Levels of the *de novo* methylating enzyme DNMT3A were unchanged, Figure 3D. Western blot analysis of hypoxic nuclear extracts showed that DNMT1 and DNMT3B protein was significantly up-regulated in hypoxia (Figure 3F), suggesting a possible role in regulating the global changes in DNA methylation in this environment. Interestingly, when examining the human cardiac tissue samples, DNMT1 and DNMT3B gene expression levels significantly correlated with CAIX levels ( $r = 0.64$ ,  $p < 0.001$ ;  $r = 0.50$ ,  $p < 0.01$ , respectively), Figure 3G and 3H.

### **Hypoxic regulation of DNA methyltransferases is mediated by HIF-1 $\alpha$ .**

The mechanism by which hypoxia regulates DNMT1 and DNMT3B expression was explored due to the importance of these maintenance and *de novo* methylating enzymes in cellular adaptation to chronic hypoxia. Following analysis of the DNMT1 and DNMT3B promoter, a consensus sequence for a HIF-1 $\alpha$  binding site, referred to as a hypoxia response element (HRE) was identified. Accordingly, this hypoxia-mediated transcription factor posed as a likely candidate for regulating DNMT expression. To investigate this further, a luciferase expression construct containing the human DNMT1 or DNMT3B promoter was generated (pDNMT1-Luc, pDNMT3B-Luc, respectively). An additional construct was generated where the HIF-1 $\alpha$  binding site was mutated (pDNMT1- $\Delta$ HRE-Luc and pDNMT3B- $\Delta$ HRE-Luc). HeLa cells were selected as a suitable vehicle to investigate hypoxic

regulation of DNMT due to their transfectability and as they possess a functional HIF-1 $\alpha$  responsive pathway when exposed to 1% hypoxia, as indicated by nuclear protein stabilization, Figure 4A. HeLa cells were transfected with either a luciferase construct with a functional or HRE mutated DNMT promoter sequence. Cells were cultured in normoxia or 1% hypoxia for 24 hours, prior to analysis of luciferase activity. Results indicate that the DNMT1 and DNMT3B promoter activity was increased by 2 to 3-fold in hypoxia ( $p<0.05$ ). Hypoxia-mediated DNMT1 and DNMT3B promoter activity was significantly attenuated when the HIF-1 $\alpha$  binding site was mutated ( $p<0.01$ ), Figure 4B and 4C.

As supportive evidence of a role for HIF-1 $\alpha$  in regulating the expression of the DNA methylation maintenance enzyme DNMT1, and the *de novo* methylating enzyme DNMT3B in hypoxia, HCF cells were treated with the prolyl hydroxylase inhibitor DMOG in normoxia. As highlighted in Figure 4D, DMOG treatment stabilizes nuclear HIF-1 $\alpha$  protein expression, and also results in increased expression of DNMT1 and DNMT3B.

Collectively, these data indicate that hypoxia-induced expression of DNMT1 and DNMT3B in cardiac fibroblast cells is at least in part regulated by the hypoxia inducible transcription factor HIF-1 $\alpha$ . The *de novo* methylating enzyme DNMT3B is the most likely candidate to be responsible for hypoxia-induced aberrant DNA hypermethylation, which is maintained by DNMT1.

#### **Targeted inhibition of DNA methyltransferases reduces the fibrotic markers collagen and alpha smooth muscle actin.**

Based on these results, we investigated the impact of reducing DNMT3B levels on the expression of fibrosis related genes. These experiments were carried out using siRNA to prevent/reduce DNMT3B expression. Human cardiac fibroblast cells were transfected with either siDNMT3B or control siRNA and were analyzed four days later using Western blotting to quantify cellular levels of collagen 1 and alpha smooth muscle actin (ASMA). siRNA targeted DNMT3B knock down resulted in a significant reduction in expression of pro-fibrotic proteins including ASMA and collagen 1 (Figure 5A-C).

Successful siRNA knockdown of DNMT3B was confirmed by Western blotting. Alpha tubulin was utilized as a loading control.

In addition to specifically targeting DNMT3B, the impact of a global DNA methylation inhibitor 5-aza 2'-deoxycytidine (5-aza) was assessed for potential anti-fibrotic properties. Treating hypoxic fibroblasts with the DNMT inhibitor 5-aza inhibited the pro-fibrotic effects of TGF $\beta$ , one of the most potent pro-fibrotic agonists. 5-aza significantly reduced expression of ASMA and collagen 1 (Figure 5D and 5E).

## Discussion

The detrimental impact of ischemia on the structure and function of the myocardium is well acknowledged. Initial cardiac responses to regional hypoxia, in the setting of coronary artery disease are likely organ protective. However, chronic insults or maladaptation can lead to reactive cardiac fibrosis that over time may potentially lead to heart failure (3, 5). The importance of this led us to investigate the relationship between myocardial tissue hypoxia and fibrosis, and to determine whether hypoxia can regulate the fibrotic phenotype in cardiac fibroblast cells. We also sought to examine whether any hypoxia-induced pro-fibrotic responses were related to changes in the epigenetic profile of cardiac fibroblast cells.

Using human cardiac tissue we were able to look at the relationship between the degree of tissue hypoxia and fibrosis. The extent of myocardial tissue hypoxia was assessed by quantifying the gene expression levels of carbonic anhydrase IX (CAIX). CAIX is involved in cell adhesion and pH regulation with its expression being controlled by hypoxia inducible factor 1 (HIF-1). The utility of CAIX as a marker of myocardial tissue hypoxia has been shown (11). In this study, CAIX was chosen as a surrogate marker of hypoxia as the surgical biopsies were processed in a way that would not have preserved HIF-1 protein stabilization.(12, 13). In support of this, we provided confirmation that CAIX is hypoxia inducible in primary human cardiac fibroblast cells, as indicated in *the in vitro* experiments (Figure 2). Analysis of the myocardial tissue highlighted a significant positive



correlation between gene expression levels of CAIX with both collagen 1 and the myofibroblast differentiation marker alpha-smooth muscle actin (ASMA). Collagen 3 gene expression did not significantly correlate, however a close relationship was observed. To further investigate this, the cardiac tissue samples were stained with Masson's trichrome blue (MTC) in order to quantify fibrillar collagen 1 protein deposition. Staining for collagen, blue in appearance, was quantified using two approaches, namely automated digital analysis which involved applying a positive pixel algorithm to quantify blue pixels within digitalized stained sections, and a manual blinded scoring method carried out by an experienced clinical Pathologist. Using the median CAIX expression level, the tissue cohort was divided into low and high CAIX expressers, signifying low and high tissue hypoxia. Using this division, the degree of collagen deposition was compared. Using automated quantification, a significantly higher level of collagen deposition was detected in the more hypoxic tissue (high CAIX) and these findings were confirmed by the blinded manual scoring.

As the main source of enhanced ASMA and collagen in hypoxic cardiac tissue is the fibroblast, we carried out *in vitro* studies utilizing human primary cardiac fibroblast cells (HCF). In order to create a model of chronic hypoxia, reflective of tissue hypoxia, cells were cultured in 1% oxygen for up to 8 days. Importantly, hypoxia stabilized HIF-1 $\alpha$  protein and up-regulated CAIX expression under these conditions demonstrating the cells were experiencing a hypoxic environment. Interestingly, we also observed an increase in cell proliferation in hypoxia, a process that could contribute to the overall fibrotic burden *in vivo*. Whilst exaggerated fibroblast proliferation is likely to contribute to the fibrotic response what is perhaps more important is the differentiation of resting fibroblasts into activated myofibroblasts. We assessed myofibroblast differentiation using ASMA and collagen 1 and report an increase in gene expression in fibroblasts exposed to chronic hypoxia (1%, 8 days). In addition to promoting myofibroblast differentiation chronic hypoxia also augmented fibroblast responses to exogenous TGF $\beta$ 1 treatment, with cells exhibiting greater levels of collagen 1 and ASMA induction. These important disease relevant observations warrant further investigations into the pro-fibrotic nature of hypoxia including the impact on matrix protein production and degradation.

Given the role of chromatin remodeling in regulating cellular phenotypes we sought to determine whether the hypoxia-induced fibrotic phenotype was dependent upon epigenetic modifications. As such, we sought to determine whether these findings occurred on a background of epigenetic changes, and thus providing a potential platform to support fibrogenesis.

The importance of epigenetics in cardiovascular disease is becoming ever apparent, with previous studies exploring the impact of histone modifications on gene expression in various cardiac diseases (14-16). However, studies involving epigenetic modifications in cardiac fibroblasts are limited, particularly investigations into DNA methylation changes and subsequent pro-fibrotic phenotypes. Given the importance of this epigenetic phenomenon, and previously published literature highlighting that hypoxia can impact the epigenetic machinery, including DNA methylation in cancer (17, 18), we examined whether hypoxia can alter the DNA methylation profile of cardiac fibroblast cells. As highlighted in Figure 3A, we found that chronic hypoxia significantly increased global DNA methylation within the genome of cardiac fibroblast cells. Subsequent analysis of the DNA methyltransferase enzymes (DNMT) revealed that both DNMT1 and DNMT3B gene and protein expression was increased, highlighting a potential mechanism by which hypoxia can hypermethylate the DNA of cardiac fibroblast cells. Interestingly, DNMT1 and DNMT3B gene expression levels within the cardiac tissue significantly correlated with CAIX levels, indicating that the *in vitro* relationship between hypoxia and DNMTs are also apparent *in vivo*.

During embryogenesis, when the methylation pattern of the genome is being established, expression levels of the *de novo* methylation enzyme DNMT3B are high. In contrast, in normal healthy adult tissue DNMT3B expression is usually low whilst DNMT1 maintains the DNA methylation pattern and phenotype of dividing cells. However, increased expression of DNMT3B has been implicated in the pathogenesis of numerous diseases, including cancer (19, 20). Therefore, the re-emergence of DNMT3B expression in disease states is likely to cause pathological DNA methylation and aberrant gene silencing. We therefore examined whether there was a direct role for DNMTs in hypoxia-mediated cardiac fibroblast differentiation and activation. Upon examination of the DNMT 1 and

DNMT3B gene, a putative hypoxia response element (HRE) was discovered in the 5'UTR, providing a mechanism by which hypoxia can drive its expression via the transcription factor HIF-1 $\alpha$ . Two approaches were undertaken to confirm this theory; (I) a study generating DNMT promoter driven luciferase constructs with either a functional (pDNMT1/3B-Luc) or mutated (pDNMT1/3B- $\Delta$ HRE-Luc) HRE site (Supplemental Material), and (II) a study using the compound DMOG to stabilize HIF-1 $\alpha$  in normoxia. As shown in Figure 4, HeLa cells transfected with either pDNMT1-Luc or pDNMT3B-Luc exhibit a significant increase in luciferase expression in hypoxia compared with cells maintained in normoxia. Importantly, when the HRE site is mutated, there is a significant blunting in luciferase activity. Of note, DNMT up-regulation is not completely abolished, suggesting the possibility that additional hypoxia-mediated transcription factors may contribute to DNMT regulation. A role for HIF-1 $\alpha$  in regulating DNMT1 and DNMT3B is further supported by the use of DMOG to inhibit prolyl hydroxylase-dependent degradation of HIF-1 $\alpha$  in normoxia.

Collectively, both approaches confirm that hypoxia-mediated up-regulation of DNMT1 and DNMT3B is regulated by the hypoxia inducible transcription factor HIF-1 $\alpha$ . Given that cellular adaptation to chronic hypoxia is a pathological feature of many inflammatory and oncogenic processes it is likely that the importance of the data presented here extends well beyond the scope of cardiac fibrosis. HIF-mediated hypoxic regulation of DNA methyltransferase enzymes and resultant DNA methylation changes is likely to be an important normal physiological mediator in response to chronic injury, as well as a pathological feature in the establishment and progression of disease.

Factors in addition to the direct hypoxic insult, that are implicated in the pathophysiology and may impact the global methylation profile, need to be considered. For example, it has been recently reported by Pan et al. that the pro-fibrotic cytokine TGF $\beta$  can directly inhibit the expression levels of DNMT1 and the de novo methyltransferase DNMT3A in neonatal rat cardiac fibroblasts. This results in hypomethylation of COL1A1 promoter and the subsequent up-regulation of collagen 1 (21). It is of interest that TGF down-regulated the expression of DNMT1 and DNMT3A, and did not impact DNMT3B expression, highlighting a TGF specific repression of methyltransferase sub-classes. Similarly, we observe hypoxia impacting DNMT1 and DNMT3B expression, whereas DNMT3A was

not affected. In addition, in the work by Pan and colleagues, down-regulation of DNMT3A alone was sufficient to hypomethylate COL1A1, whilst still in the presence of unaltered DNMT3B expression levels. Collectively this suggests that possible distinct roles for DNMT3A and DNMT3B in the pathogenesis of cardiac fibrosis may emerge.

Within our study we observe a hypoxia-induced net global DNA hypermethylation state, although it is likely that both gene-specific hypo and hypermethylation changes are occurring within a hypoxic environment, similar to those observed in cancer. A study exploring gene-specific changes within hypoxic cardiac tissue warrants investigation. Several mechanisms could account for our observations, for example, it is possible that the methylation status of collagen repressors, such as FLI-1, could become hypermethylated in the ischemic heart (22), or that the collagen promoter region itself could become hypomethylated despite apparent global hypermethylation. Additional fibrotic relevant genes already reported to be influenced by epigenetic medications are reviewed elsewhere (9). It is also possible that cumulative hypoxic insults on the heart over the life time of a person could influence the methylation status of the heart, and may impact the likelihood or rate of myocardial disease development. In fact, even brief exposure to hypoxia in-utero may affect the methylation profile within the myocardium, which could persist to adulthood. For example, an intriguing study carried out by Patterson and colleagues looked at the impact of maternal hypoxia on the methylation status of cardiac genes in the fetus, and in the hearts of the adult offspring. Exposing pregnant rats to 10.5% oxygen between days 15 and 21 of gestation resulted in the PKC $\epsilon$  gene within the fetal hearts becoming hypermethylated and this epigenetic mark was maintained in adulthood (23). Additional environmental stimuli for causing aberrant DNA hypermethylation of the PKC $\epsilon$  gene within the heart have been reported by Meyer and colleagues (24). The functional importance of this gene in cardiac fibrosis and diastolic dysfunction has been reported previously (25). Epigenetic mechanisms by which external factors can impact the expression levels of genes within the myocardium is an important area of research and will yield new insights into disease pathogenesis, which have the potential to be modified using epigenetic based therapeutic approaches. In addition to our reported alterations in DNA methylation it is also fundamental that we highlight the significance of other epigenetic phenomena that likely contribute to our findings, in particular the role of histone

modifications. Several publications have documented the role of histone modifications in the pathogenesis of fibrotic diseases, and the potential therapeutic role of histone modifying drugs for the treatment of such conditions (9). Expanding research into the area of hypoxia induced histone modifications in cardiac fibrosis would be of great value and scientific insight.

Having shown that hypoxia is associated with a pro-fibrotic fibroblast phenotype, which occurs against a background of epigenetic changes, including HIF-1 $\alpha$  mediated up-regulation of the *de novo* methylating enzyme DNMT3B, we sought to determine whether a DNMT3B targeted approach could be potentially anti-fibrotic. siRNA knock-down of DNMT3B expression in human primary cardiac fibroblasts resulted in a reduction in both collagen 1 and ASMA expression, thus providing evidence that DNMT3B represents a potentially useful therapeutic target in the treatment of fibrotic diseases. Investigating the impact of down-regulating DNMT1 would be of experimental interest and may provide additional fibrotic modulating activity. The potential value of targeting DNMT enzymes in cardiac fibrosis was supported by evidence that 5-aza inhibits the induction of a myofibroblast phenotype. Further work exploring this observation is required, including assessment of the anti-fibrotic potential of 5-aza using additional experimental approaches.

These data suggest that changes in DNA methylation play an important role in cardiac fibroblast function in hypoxia, contributing to the fibrotic burden. Whether these changes in DNA methylation are directly involved in the enhanced fibrotic response *in vivo* requires further investigation. However, we have taken the first steps to explore this by using ex-vivo human tissue and highlighted an important association with degree of tissue hypoxia and levels of collagen and DNA methyltransferase enzymes.

## Methods

### Human cardiac tissue collection and handling.

Human tissue samples were collected from the hearts of 26 stable patients undergoing elective cardiac-bypass surgery. Specifically, right atrial appendages were obtained adjacent to the venous cannulation site. The surgical indication included elective coronary artery bypass grafting (n=18) and

elective valve repair/replacement (n=8). All subjects gave written informed consent to participate in the study. The study protocol conformed to the principles of the Helsinki Declaration and received local ethical committee approval. Demographic and clinical details of this patient cohort are highlighted in Table 1. Tissue samples were collected at onset of surgery and immediately divided into two parts and either stored in Allprotect Tissue Stabilization Reagent (Qiagen) for subsequent RNA extraction, or formalin-fixed for histological staining.

### **Cardiac tissue analysis.**

For analysis of gene expression within the myocardial samples, the tissue was first individually disrupted and homogenized using an Ultra Turrax T25 Dispersing Instrument (IKA) before the RNA was extracted using the AllPrep DNA/RNA extraction kit (Qiagen), according to the manufacturer's instructions. First strand cDNA synthesis was carried out using SuperScript II RT (Invitrogen). Quantitative real-time PCR (QPCR) primers were designed so that one of each primer pair was exon/exon boundary spanning to ensure only mature mRNA was amplified. The sequences of the gene-specific primers used are as follows; ASMA, 5'-CGTTACTACTGCTGAGCGTGA-3' (forward), 5'-AACGTTTCATTTCCGATGGTG-3' (reverse); collagen 1  $\alpha$ 1 (COL1A1), 5'-GAACGCGTGTTCATCCCTTGT-3' (forward), 5'-GAACGAGGTAGTCTTTCAGCAACA-3' (reverse); collagen 3  $\alpha$ 1 (COL3A1), 5'-AACACGCAAGGCTGTGAGACT-3' (forward), 5'-GAACGAGGTAGTCTTTCAGCAACA-3' (reverse); carbonic anhydrase IX (CAIX), 5'-AGGTCCCAGGACTGGACATA-3' (forward), 5'-GAGGGTGTGGAGCTGCTTAG-3' (reverse); DNMT1, 5'-TATCCGAGGAGGGCTACCTG-3' (forward), 5'-CACTTCCCGGTTGTAAGCAT-3' (reverse); DNMT3A, 5'-AGCCCAAGGTCAAGGAGATT-3' (forward), 5'-GTTCTTGCAAGTTTGGCACA-3' (reverse); DNMT3B, 5'-TCAGGATGGGAAGGAGTTTG-3' (forward), 5'-CTGCAGAGACCTCGGAGAAC-3' (reverse). QPCR reactions were normalized by amplifying the same cDNA with beta-2-microglobulin (B2M) primers, 5'-AGGCTATCCAGCGTACTCCA-3' (forward), 5'-CCAGTCCTTGCTGAAAGACA-3' (reverse).

QPCR was performed using Platinum SYBR Green qPCR SuperMix-UDG (Invitrogen).

Amplification and detection were carried out using Mx3000P System (Stratagene). The PCR cycling program consisted of 40 three-step cycles of 15 seconds/95°C, 30 seconds/ $T_A$  and 30 seconds/72°C.

Each sample was amplified in duplicate. In order to confirm signal specificity, a melting program was carried out after the PCR cycles were completed.

For analysis of interstitial collagen within the myocardial sample, formalin-fixed tissue was paraffin-embedded and stained using a Masson's trichrome (MTC) Stain Kit (Dako) optimised for use on an Artisan staining system according to the manufacturer's instructions. In brief, 8µm thick sections of myocardial tissue were deparaffinised, rehydrated, and incubated over night in Bouin's solution. The next day sections were incubated with the following reagents; Weigert's haematoxylin, Biebrich Scarlet-acid Fuchsin solution, Phosphotungstic/ Phosphomolybdic acid solution, Aniline Blue solution. Following this, tissue sections were incubated in acetic acid, and subsequently dehydrated using an alcohol gradient to xylene and coverslipped ready for histological analysis.

#### **Manual scoring of MTC stained cardiac biopsies.**

Microscope slides containing 8µm thick sections of myocardial tissue stained with MTC were examined by a pathologist (OS) and manually assessed for the degree of fibrosis in a blinded fashion. MTC for collagen type I detection (fibrosis) was graded from 0 to 5, where 0 is the least and 5 is the most severe interstitial fibrosis.

#### **Automated image analysis of MTC stained cardiac biopsies.**

The Aperio ScanScope XT Slide Scanner (Aperio Technologies) system was used to capture whole slide digital images with a 20x objective. Automated image analysis was performed using Imagescope (Aperio). A positive pixel count algorithm was used to automatically quantify the area occupied by stain colors within each scanned slide image. Calibration of individual staining patterns was performed by specifying the requisite color (range of hues and saturation) and limits for the desired intensity range. Required input parameters for each stain were based on the HSI (Hue,

Saturation and Intensity) color model. To detect the blue color of collagen with MTC stain, a hue value of 0.66 was specified. The equivalent value for detection of red stained myocytes was 0.0. The default hue width value of 0.5 was used to allow inclusion of a moderate range of color shades. A collagen volume fraction was calculated based on the percent of blue collagen staining quantified within a tissue section.

### **Primary cell culture.**

Human primary cardiac fibroblast cells from the adult ventricle (HCF) were purchased from ScienCell Research Laboratories. Primary cells were derived from a single female donor aged 20. Cells between passage 6 and 12 were used for experiments. Of note, for these primary cells, cellular proliferation began to slow from passage 20 onwards. Until required for experiments, cells were cultured and maintained in Dulbecco's modified eagles medium (DMEM) (Gibco), supplemented with 10% Fetal Bovine Serum (Gibco) and penicillin-streptomycin antibiotics (Gibco) in a 5% CO<sub>2</sub> humidified incubator kept at 37°C.

### **Cell culture treatments.**

Where indicated, HCF cells were exposed to a 1% oxygen environment for up to 8 days using a hypoxic chamber (Coy Laboratories). The effects of 10ng/ml recombinant TGFβ1 treatment (R&D Systems) under these conditions were investigated. When required, cells were treated for up to 72 hours with 1mM of the prolyl hydroxylase inhibitor (DMOG) (Sigma) to simulate hypoxia through the induction of HIF under normoxic conditions.

### **Quantitative Flow Cytometry.**

The impact of hypoxia on the global DNA methylation profile in HCF cells was investigated using an antibody specific to methylated DNA and quantified using flow cytometry as previously described (17, 26, 27). Briefly, HCF cells exposed to either normoxia (21% oxygen) or hypoxia (1% oxygen) were fixed in Carnoy's solution prior to 60 minutes acid hydrolysis in 1M HCl at 37°C. Following this DNA denaturation step, cells were immunostained using anti-5-methylcytidine (5MeC) monoclonal



antibody (Eurogentec). IgG1 negative controls were used at the same concentration as the primary antibody. Secondary immunostaining was conducted using an FITC conjugated rabbit anti-mouse secondary antibody (Dako). Analysis was performed on a CYAN flow cytometer and results assessed using SUMMIT software (Dako).

### **Quantitative real-time PCR analysis of primary HCF cells.**

Gene expression changes were measured in HCF cells using QPCR as described in human cardiac tissue analysis methods section. RNA isolation from cells was achieved using NucleoSpin RNA II Kit (Macherey-Nagel). QPCR data was analysed using the delta delta CT method.

### **Western Blotting.**

Whole cell protein lysates were generated using RIPA Lysis Buffer (Millipore), containing a protease inhibitor cocktail (Roche). Nuclear protein extracts were obtained using the Ne-PeR Nuclear and Cytoplasmic extraction Reagents, according to manufacturer's instructions (Pierce Biotechnology). Protein concentrations were determined using the BCA Protein Assay Kit (Pierce). 10-20µg of protein lysates were denatured, reduced and resolved on SDS-polyacrylamide gels by SDS-PAGE before transfer onto 0.45µm pore size Immobilon-P polyvinylidene fluoride (PVDF) membranes (Millipore).

Membranes were incubated with blocking buffer (TBS, 0.25% Tween-20, 0.1% serum from species that secondary antibody was raised in, and 5% fat free skimmed milk) for 1 hour at room temperature. Membranes were subsequently probed overnight with either anti-ASMA (Sigma), anti-collagen 1 (Santa Cruz), anti-DNMT3B (Imgenex), anti-DNMT1 (Imgenex), or anti-hypoxia inducible factor 1α (HIF-1α) (Novus Biologicals). Detection of the specific binding of the primary antibody was achieved using HRP-conjugated secondary antibodies, followed by signal detection with Immobilon Western chemiluminescent HRP substrate (Millipore) according to the manufacturer's instructions. Either anti-lamin A/C or anti-alpha tubulin (Sigma) were used to verify equal loading.

### **Generating a functional and mutated DNMT3B and DNMT1 luciferase construct.**

A 258bp fragment of the DNMT3B promoter containing a putative hypoxia response element (HRE) was cloned and inserted into a pGL3 luciferase construct (Promega), generating pDNMT3B-Luc (28). Similarly, a 732bp fragment of the DNMT1 promoter containing a putative HRE was cloned and inserted into pGL3 luciferase, generating pDNMT1-Luc(29). In addition, a mutated version of both constructs was created by site-directed mutagenesis using QuikChange II Site-Directed Mutagenesis Kit (Stratagene) to mutate the putative HRE within the DNMT promoters. Specifically, for DNMT3B two cytosine bases within the putative HRE were replaced with adenine bases, generating pDNMT3B-ΔHRE-Luc, and for DNMT1 an adenine base and a cytosine base were replaced with a thymine and an adenine, respectively, generating pDNMT1-ΔHRE-Luc. For more specific details please see Supplemental Material. DNA sequencing was used to confirm the presence of the mutation. Either pDNMT3B-Luc, pDNMT3B-ΔHRE-Luc, pDNMT1-Luc, pDNMT1-ΔHRE-Luc, or empty vector was subsequently transiently transfected into Hela cells using FUGENE HD (Promega). 24 hours post transfection, cells were either exposed to 1% oxygen for 24 hours, or left in normoxia (21% oxygen). The degree of DNMT3B and DNMT1 promoter activity was quantified using the luciferin/luciferase bioluminescence assay following cell lysis with Passive Lysis Buffer (Promega) and incubating with Luciferase Assay Reagent (Promega), with luciferase activity measured on a GloMax 20/20 Luminometer (Promega).

### **siRNA targeted DNMT3B knock down.**

HCF cells were transfected with either siDNMT3B or control siRNA using DharmaFect4 transfection reagent (Dharmacon). The siRNA gene sequence used to specifically target DNMT3B was 5'-AGATGACGGATGCCTAGAGTT-3'. siControl was purchased from Dharmacon (ON-TARGET plus Nontargeting siRNA #2). Transfected cells were incubated for 6 hours, replenished with fresh cell culture medium, and assessed for changes in protein expression 48 hours later using Western blotting.

**Global DNA demethylation with 5-aza-2'-deoxycytidine.**

For demethylation analysis, cells were treated with 1  $\mu$ M 5-aza-2'-deoxycytidine (5-azadC; Sigma) for up to eight days. The effect of global DNA methylation inhibition on TGF $\beta$  induction of pro-fibrotic genes was assessed.

**Statistical analysis.**

Data are represented as either the mean  $\pm$  SEM or median (interquartile range) for normally and non-normally distributed continuous variables, respectively, whereas frequencies and percentages (in parentheses) summarize categorical variables. Group comparisons were made using the two-sample independent t-test,  $\chi^2$  test, and Mann-Whitney test where appropriate. Spearman rank order correlations were performed to assess relationships between non-normally distributed variables. Statistical analysis was performed using the statistical software package GraphPad Prism.  $p < 0.05$  was deemed statistically significant.

**Funding**

This work was supported by University College Dublin, SMMS Research Support Scheme (to C.W.) and Science Foundation Ireland (to J.B.).

**Acknowledgments**

The authors would like to thank Mr. Michael Tolan for the cardiac tissue procurement.

**Conflict of interest statement**

Authors C.W., M.L., K.M., and J.B., have a pending patent application part based on this work.

## References

- 1 Kong, P., Christia, P. and Frangogiannis, N.G. (2013) The pathogenesis of cardiac fibrosis. *Cellular and molecular life sciences : CMLS*, in press.
- 2 Swynghedauw, B. (1999) Molecular mechanisms of myocardial remodeling. *Physiological reviews*, **79**, 215-262.
- 3 van den Borne, S.W., Diez, J., Blankesteijn, W.M., Verjans, J., Hofstra, L. and Narula, J. (2010) Myocardial remodeling after infarction: the role of myofibroblasts. *Nat Rev Cardiol*, **7**, 30-37.
- 4 Barallobre-Barreiro, J., Didangelos, A., Schoendube, F.A., Drozdov, I., Yin, X., Fernandez-Caggiano, M., Willeit, P., Puntmann, V.O., Aldama-Lopez, G., Shah, A.M. *et al.* (2012) Proteomics analysis of cardiac extracellular matrix remodeling in a porcine model of ischemia/reperfusion injury. *Circulation*, **125**, 789-802.
- 5 Opie, L.H., Commerford, P.J., Gersh, B.J. and Pfeffer, M.A. (2006) Controversies in ventricular remodelling. *Lancet*, **367**, 356-367.
- 6 Gabrielsen, A., Lawler, P.R., Yongzhong, W., Steinbruchel, D., Blagoja, D., Paulsson-Berne, G., Kastrup, J. and Hansson, G.K. (2007) Gene expression signals involved in ischemic injury, extracellular matrix composition and fibrosis defined by global mRNA profiling of the human left ventricular myocardium. *J. Mol. Cell .Cardiol.*, **42**, 870-883.
- 7 Egger, G., Liang, G., Aparicio, A. and Jones, P.A. (2004) Epigenetics in human disease and prospects for epigenetic therapy. *Nature*, **429**, 457-463.
- 8 Sharma, S., Kelly, T.K. and Jones, P.A. (2010) Epigenetics in cancer. *Carcinogenesis*, **31**, 27-36.
- 9 Robinson, C.M., Watson, C.J. and Baugh, J.A. (2012) Epigenetics within the matrix: a neo-regulator of fibrotic disease. *Epigenetics*, **7**, 987-993.
- 10 Papait, R., Greco, C., Kunderfranco, P., Latronico, M.V. and Condorelli, G. (2013) Epigenetics: a new mechanism of regulation of heart failure? *Basic Res. Cardiol.*, **108**, 361.
- 11 Holotnakova, T., Ziegelhoffer, A., Ohradanova, A., Hulikova, A., Novakova, M., Kopacek, J., Pastorek, J. and Pastorekova, S. (2008) Induction of carbonic anhydrase IX by hypoxia and chemical disruption of oxygen sensing in rat fibroblasts and cardiomyocytes. *Pflugers Arch.*, **456**, 323-337.

- 12 Ivan, M., Kondo, K., Yang, H., Kim, W., Valiando, J., Ohh, M., Salic, A., Asara, J.M., Lane, W.S. and Kaelin, W.G., Jr. (2001) HIFalpha targeted for VHL-mediated destruction by proline hydroxylation: implications for O<sub>2</sub> sensing. *Science*, **292**, 464-468.
- 13 Jaakkola, P., Mole, D.R., Tian, Y.M., Wilson, M.I., Gielbert, J., Gaskell, S.J., Kriegsheim, A., Hebestreit, H.F., Mukherji, M., Schofield, C.J. *et al.* (2001) Targeting of HIF-alpha to the von Hippel-Lindau ubiquitylation complex by O<sub>2</sub>-regulated prolyl hydroxylation. *Science*, **292**, 468-472.
- 14 Lorenzen, J.M., Martino, F. and Thum, T. (2012) Epigenetic modifications in cardiovascular disease. *Basic Res. Cardiol.*, **107**, 245.
- 15 Ordovas, J.M. and Smith, C.E. (2010) Epigenetics and cardiovascular disease. *Nat. Rev. Cardiol.*, **7**, 510-519.
- 16 Han, P., Hang, C.T., Yang, J. and Chang, C.P. (2011) Chromatin remodeling in cardiovascular development and physiology. *Circ. Res.*, **108**, 378-396.
- 17 Watson, J.A., Watson, C.J., McCrohan, A.M., Woodfine, K., Tosetto, M., McDaid, J., Gallagher, E., Betts, D., Baugh, J., O'Sullivan, J. *et al.* (2009) Generation of an epigenetic signature by chronic hypoxia in prostate cells. *Hum. Mol. Genet.*, **18**, 3594-3604.
- 18 Watson, J.A., Watson, C.J., McCann, A. and Baugh, J. (2010) Epigenetics, the epicenter of the hypoxic response. *Epigenetics*, **5**, 293-296.
- 19 Roll, J.D., Rivenbark, A.G., Jones, W.D. and Coleman, W.B. (2008) DNMT3b overexpression contributes to a hypermethylator phenotype in human breast cancer cell lines. *Molecular cancer*, **7**, 15.
- 20 Robertson, K.D., Uzvolgyi, E., Liang, G., Talmadge, C., Sumegi, J., Gonzales, F.A. and Jones, P.A. (1999) The human DNA methyltransferases (DNMTs) 1, 3a and 3b: coordinate mRNA expression in normal tissues and overexpression in tumors. *Nucleic acids research*, **27**, 2291-2298.
- 21 Pan, X., Chen, Z., Huang, R., Yao, Y. and Ma, G. (2013) Transforming growth factor beta1 induces the expression of collagen type I by DNA methylation in cardiac fibroblasts. *PloS one*, **8**, e60335.

- 22 Wang, Y., Fan, P.S. and Kahaleh, B. (2006) Association between enhanced type I collagen expression and epigenetic repression of the FLII gene in scleroderma fibroblasts. *Arthritis Rheum.*, **54**, 2271-2279.
- 23 Patterson, A.J., Chen, M., Xue, Q., Xiao, D. and Zhang, L. (2010) Chronic prenatal hypoxia induces epigenetic programming of PKC{epsilon} gene repression in rat hearts. *Circ. Res.*, **107**, 365-373.
- 24 Meyer, K., Zhang, H. and Zhang, L. (2009) Direct effect of cocaine on epigenetic regulation of PKCepsilon gene repression in the fetal rat heart. *J. Mol. Cell. Cardiol.*, **47**, 504-511.
- 25 Klein, G., Schaefer, A., Hilfiker-Kleiner, D., Oppermann, D., Shukla, P., Quint, A., Podewski, E., Hilfiker, A., Schroder, F., Leitges, M. *et al.* (2005) Increased collagen deposition and diastolic dysfunction but preserved myocardial hypertrophy after pressure overload in mice lacking PKCepsilon. *Circ. Res.*, **96**, 748-755.
- 26 Watson, C.J., O'Kane, H., Maxwell, P., Sharaf, O., Petak, I., Hyland, P.L., O'Rourke, D., McKnight, J., Canning, P. and Williamson, K. (2012) Identification of a methylation hotspot in the death receptor Fas/CD95 in bladder cancer. *Int. J. Oncol.*, **40**, 645-654.
- 27 Robinson, C.M., Neary, R., Levendale, A., Watson, C.J. and Baugh, J.A. (2012) Hypoxia-induced DNA hypermethylation in human pulmonary fibroblasts is associated with Thy-1 promoter methylation and the development of a pro-fibrotic phenotype. *Respiratory research*, **13**, 74.
- 28 Mei, C., Sun, L., Liu, Y., Yang, Y., Cai, X., Liu, M., Yao, W., Wang, C., Li, X., Wang, L. *et al.* (2010) Transcriptional and post-transcriptional control of DNA methyltransferase 3B is regulated by phosphatidylinositol 3 kinase/Akt pathway in human hepatocellular carcinoma cell lines. *Journal of cellular biochemistry*, **111**, 158-167.
- 29 Novakovic, B., Wong, N.C., Sibson, M., Ng, H.K., Morley, R., Manuelpillai, U., Down, T., Rakyan, V.K., Beck, S., Hiendleder, S. *et al.* (2010) DNA methylation-mediated down-regulation of DNA methyltransferase-1 (DNMT1) is coincident with, but not essential for, global hypomethylation in human placenta. *The Journal of biological chemistry*, **285**, 9583-9593.

## Figure Legends

### **Figure 1. Tissue hypoxia is associated with an enhanced fibrotic expression profile.**

Human cardiac tissue (n=26) was obtained from cardiac by-pass patients. Collected samples were immediately divided into two parts, one for gene expression analysis and the other for histological staining. Quantitative real time PCR was used for gene expression analysis. Within human cardiac tissue, the hypoxia marker CAIX significantly correlated with gene expression of ASMA (**A**) and collagen 1 (**B**). Collagen 3 gene expression was not statistically associated with changes in CAIX expression (**C**). Panel **D** from left to right highlight examples of increased collagen deposition within the interstitium (top) and perivascular (bottom) in cardiac tissue stained with Masson's trichrome (MTC). The blue staining of the cardiac tissue represents collagen. Collagen deposition was quantified using automated positive pixel analysis of digitally scanned slides (**E** and **G**) using an Aperio ScanScope XT Slide Scanner and Imagescope software analysis (Aperio), as well as manually graded by a pathologist (**F** and **H**). The relationship between collagen deposition and hypoxia was assessed by dividing the MTC slides into two groups based on median CAIX gene expression levels. Using both methodologies increased tissue hypoxia (higher CAIX expression) was associated with a significant increase in collagen deposition ( $p<0.05$ ). Data presented in bar charts as mean  $\pm$  SEM.  $*p<0.05$ .

**Figure 2. Hypoxia induces a pro-fibrotic state in cardiac fibroblasts.** Primary human cardiac fibroblast cells were exposed to 1% hypoxic environment for up to 8 days to assess the pro-fibrotic impact of hypoxia. Chronic hypoxic exposure resulted in HIF-1 $\alpha$  protein stabilization (**A**), increased the expression of the hypoxia surrogate marker CAIX (**B**), and increased cell proliferation (**C**). Gene expression levels of alpha smooth muscle actin (ASMA) (**D**) and collagen 1 (**E**) were significantly upregulated following 4 and 8 days exposure to hypoxia compared to normoxic controls. Hypoxic fibroblasts exhibited an enhanced response to the pro-fibrotic cytokine TGF $\beta$  (**F** and **G**). Both ASMA and collagen 1 gene induction by TGF $\beta$  was significantly magnified under hypoxic conditions. All experiments  $\geq n=3$ ). Data represent mean  $\pm$  SEM.  $*p<0.05$ ,  $**p<0.01$ ,  $***p<0.001$ .

**Figure 3. Hypoxia causes DNA hypermethylation and increased DNA methyltransferase expression in cardiac fibroblasts.** Hypoxia induced epigenetic changes were assessed in primary human cardiac fibroblast cells through the study of DNA methylation. Results indicate that global DNA methylation was enhanced in cardiac fibroblast cells exposed to a chronic hypoxic environment (1% oxygen for up to 8 days), as determined using an antibody specific to DNA methylation (anti-5MeC) and flow cytometry (**A**),  $n=6$ . Immunofluorescence confirmed the nuclear specificity of the anti-5MeC antibody (**B**). DNA hypermethylation in hypoxia occurred against a background increase in DNA methyltransferase (DNMT) enzyme expression. Gene and protein expression of both DNMT1 (**C** and **F**), and DNMT3B (**E** and **F**) were significantly elevated in hypoxia,  $n=3$ . DNMT 3A levels were unchanged (**D**). Within human cardiac tissue samples ( $n=26$ ), gene expression levels of DNMT1 and DNMT3B significantly correlated with expression levels of the hypoxia marker CAIX (**G** and **H**). Data presented in bar charts as mean  $\pm$ SEM. \*\* $p<0.01$ , \*\*\* $p<0.001$ .

**Figure 4. Hypoxic regulation of DNA methyltransferase enzymes is mediated by Hypoxia Inducible Factor (HIF).** DNMT1 and DNMT3B gene promoter regions contain a consensus sequence for a HIF-1 $\alpha$  binding hypoxia response element (HRE). Promoter studies were carried out using luciferase expression constructs containing either DNMT1 or DNMT3B promoter (pDNMT1/3B-Luc) or a mutated construct with the HIF-1 $\alpha$  binding site mutated (pDNMT1/3B- $\Delta$ HRE-Luc), see Methods and Supplemental Material. Hela cells were transfected and exposed to 1% hypoxia, prior to analysis of luciferase activity. Under these hypoxic conditions HIF-1  $\alpha$  protein expression was stabilized in Hela cells (**A**). Compared to promoter activity under normoxic conditions, DNMT1 and DNMT3B promoter activity was increased 2-3 fold in hypoxia (**B** and **C**). Hypoxia-mediated DNMT 1 and DNMT3B promoter activity was significantly attenuated when the HIF-1 $\alpha$  binding site was mutated,  $n=6$ . Stabilizing HIF-1 $\alpha$  protein in human cardiac fibroblasts cells under normoxic conditions using the prolyl hydroxylase inhibitor DMOG resulted in a significant increase in DNMT1 and DNMT3B protein expression (**D**),  $n=3$ . Data presented in bar charts as mean  $\pm$ SEM. \*\* $p<0.01$ .



**Figure 5. Targeted inhibition of DNA methyltransferase (DNMT) enzymes reduces the fibrotic markers collagen and alpha smooth muscle actin.** The impact of reducing DNMT levels on the expression of fibrosis related genes was investigated using primary human cardiac fibroblast cells. Cardiac fibroblasts were assessed 48 hours after transfection with siRNA to target the *de novo* methylating enzyme DNMT3B. DNMT3B knock down resulted in a significant decrease in protein expression of collagen 1 and ASMA (**A-C**), n=4. Treatment with the global DNA methylation inhibitor 5-aza-2-deoxycytidine (5-aza) significantly reduced TGF $\beta$  induction of ASMA and collagen 1 gene expression (**D and E**), n=3. Data presented in bar charts as mean  $\pm$ SEM. \*p<0.05, \*\*p<0.01.

**Table 1. Patient Demographics.**

Characteristics of the patients from whom cardiac tissue was obtained are summarized in Table 1.

Relative tissue hypoxia was determined based on above and below the median gene expression levels of the hypoxic marker CAIX.

	Total	High tissue	Low tissue
Demographics	Population	CAIX	CAIX
N	26	13	13
Age, yr	72 ± 10	72 ± 9	72 ± 11
Gender, male	18 (69%)	9 (69%)	9 (69%)
SBP, mmHg	134 ± 6	134 ± 6	132 ± 7
DBP, mmHg	78 ± 7	76 ± 6	80 ± 7
BMI, kg/m <sup>2</sup>	27 ± 3	27 ± 3	27 ± 3
Atrial Fibrillation	5 (19%)	2 (15%)	3 (23%)
Diabetes Mellitus	5 (19%)	3 (23%)	2 (15%)
Smoking History	10 (38%)	7 (54%)	3 (23%)
Hypercholesterolemia	9 (35%)	6 (46%)	3 (23%)
Coronary Artery Disease	20 (77%)	10 (77%)	10 (77%)
Valvular Heart Disease	12 (46%)	5 (38%)	7 (54%)
Hypertension	9 (35%)	4 (31%)	5 (38%)
RAAS Inhibitor	12 (41%)	6 (46%)	6 (46%)
Beta-Blocker	16 (55%)	9 (69%)	7 (54%)
Statin	16 (55%)	11 (85%) *	5 (38%)
Creatinine, µmol/l	90 ± 13	90 ± 4	90 ± 17
BNP, pg/ml	104 (17:127)	84 (15:116)	135 (26:171)
LVEF, %	60 ± 7	60 ± 7	60 ± 8
LVIDd, mm	53.0 ± 5.0	53.0 ± 4.8	55.0 ± 5.2
IVS, mm	9.7 ± 1.5	9.6 ± 1.3	9.9 ± 1.7

PW, mm	10.7 ± 1.6	10.5 ± 2.0	11.0 ± 1.1
E/e'	8.7 ± 2.8	8.7 ± 3.0	8.6 ± 2.6
LAVI, mls/m <sup>2</sup>	28.4 ± 4.4	28.1 ± 5.2	28.6 ± 3.4

Values are mean ± SD, median (25<sup>th</sup>:75<sup>th</sup> percentiles) or n (%). SBP/DBP, systolic and diastolic blood pressure; BMI, body mass index; RAAS Inhibitor, renin angiotensin system inhibitor; BNP, b-type natriuretic peptide; LVEF, left ventricular ejection fraction; LVIDd, left ventricular end diastolic dimension; IVS, intraventricular septum; PW, posterior wall; E/e', ratio of mitral early diastolic flow velocity over tissue Doppler lateral mitral annular lengthening velocity; LAVI, left atrial volume index. \*p<0.05 high v low tissue CAIX.

## Abbreviations

5MeC: 5-methylcytosine

ASMA: alpha smooth muscle actin

CAIX: carbonic anhydrase IX

DNMT: DNA methyltransferase

ECM: extracellular matrix

HCF: Primary human cardiac fibroblast cells

HIF: hypoxia inducible factor

HRE: hypoxia response element

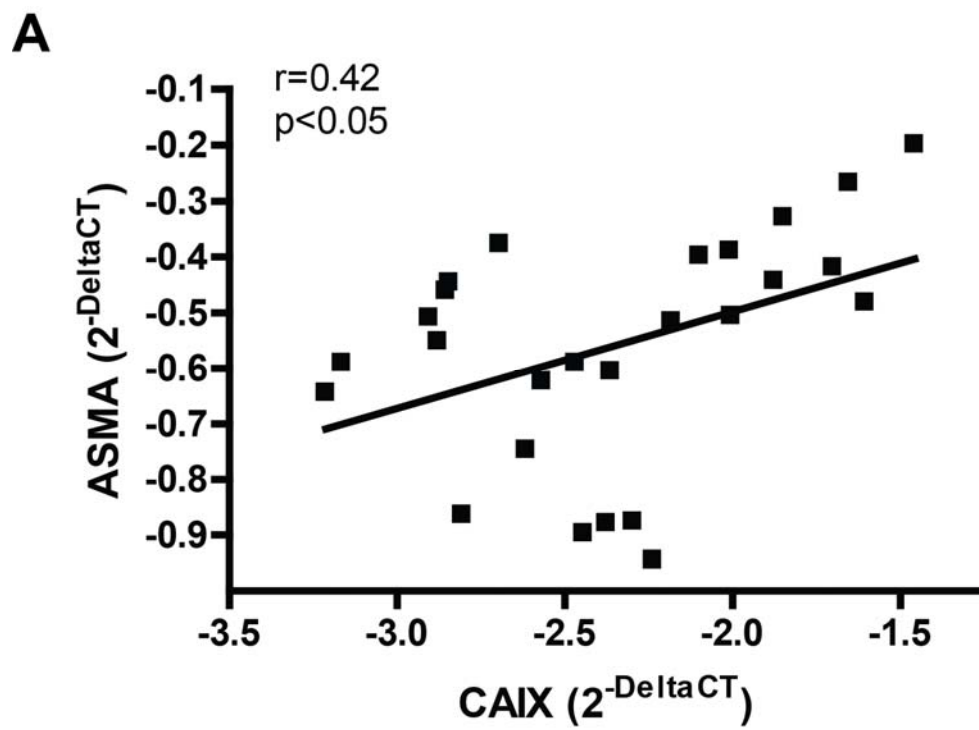
MMP: matrix metalloproteinase

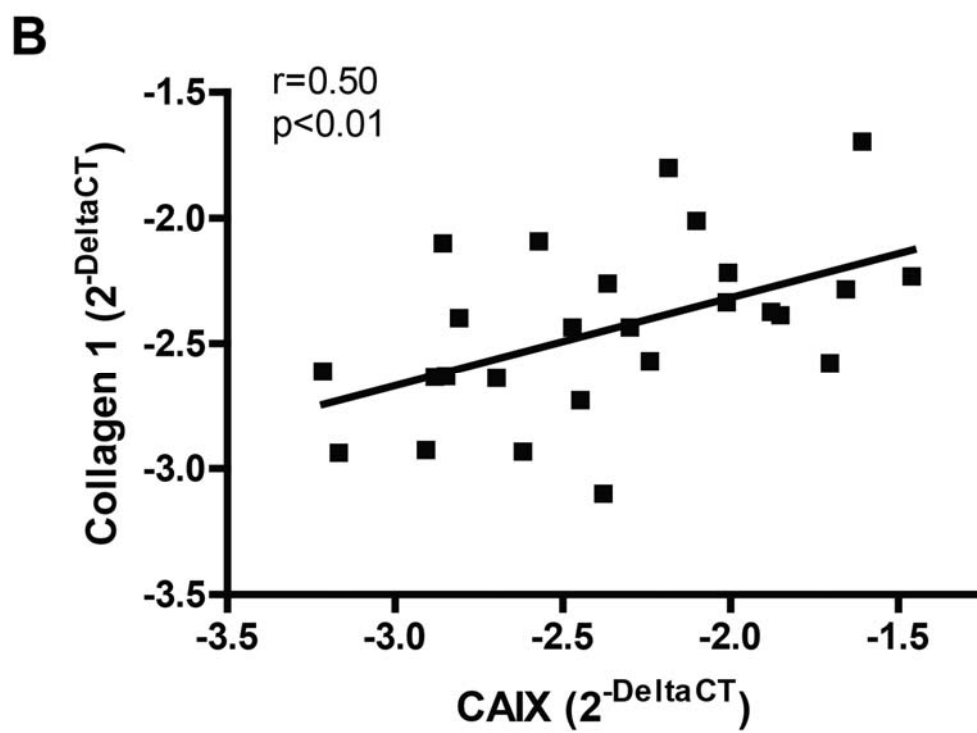
MTC: Masson's trichrome stain

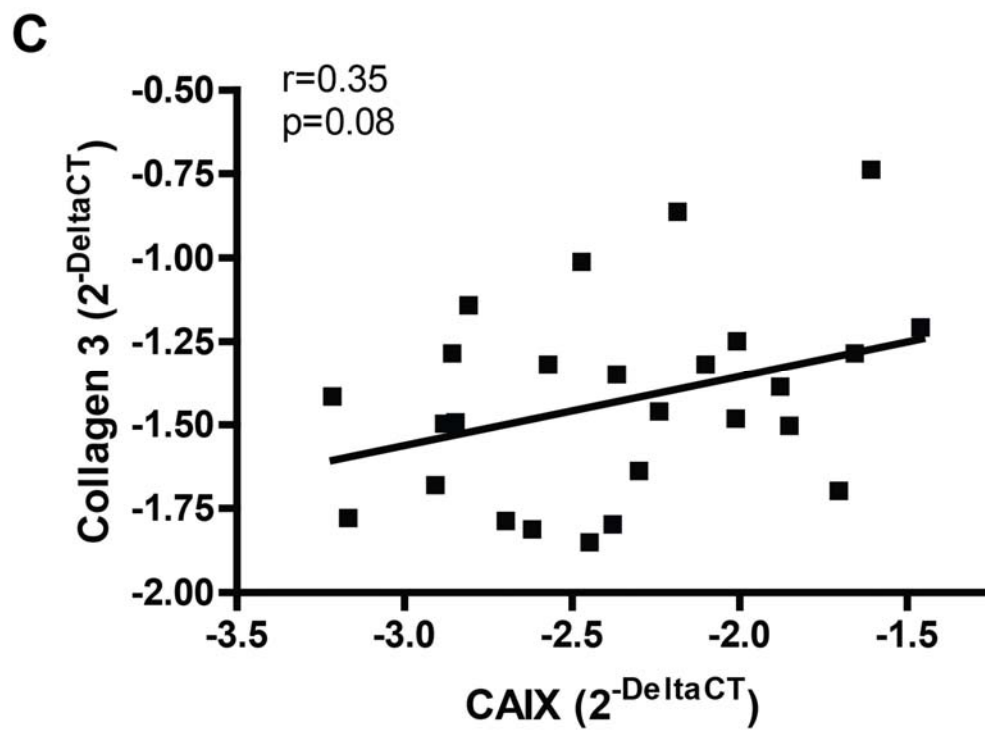
QPCR: quantitative real-time PCR

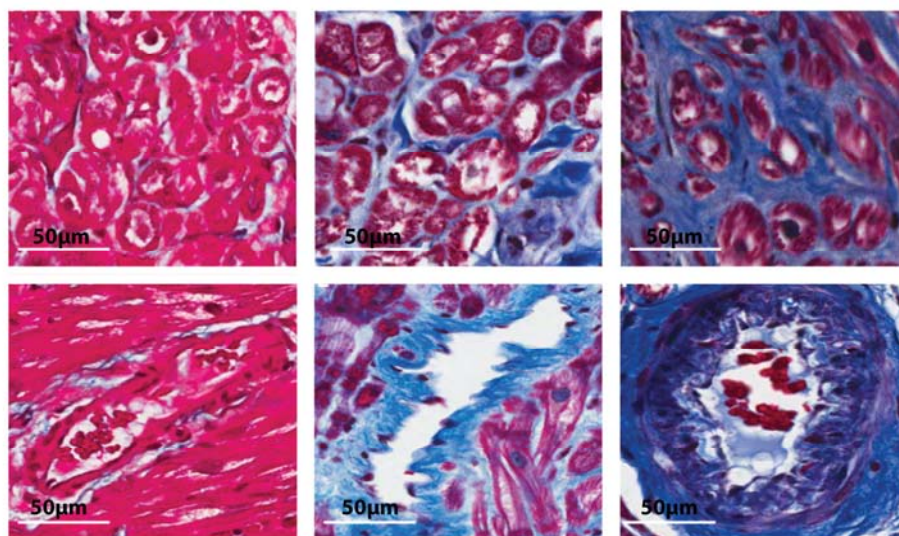
TGFβ: Transforming growth factor beta

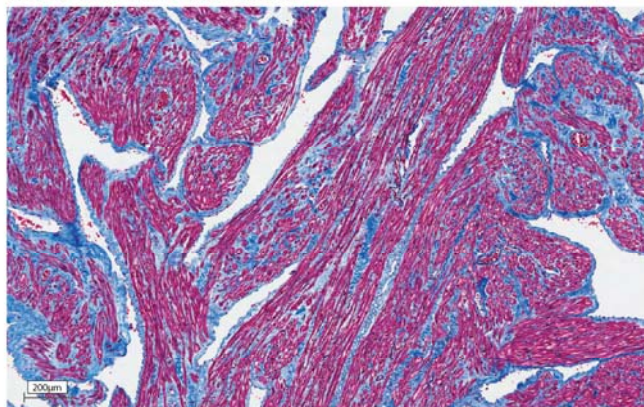
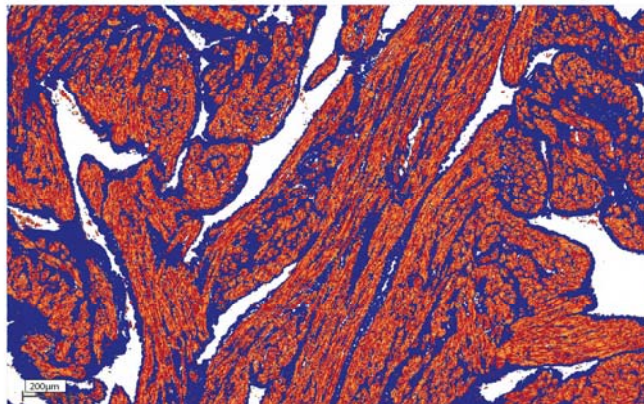
5-aza: 5-aza-2'-deoxycytidine



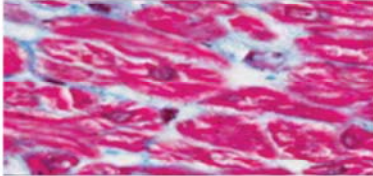
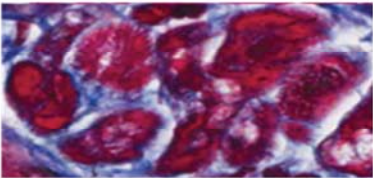
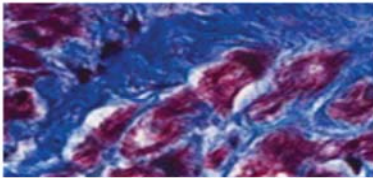
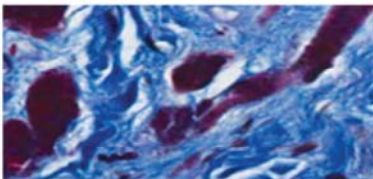
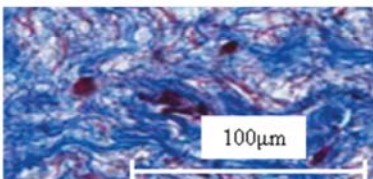




**D**

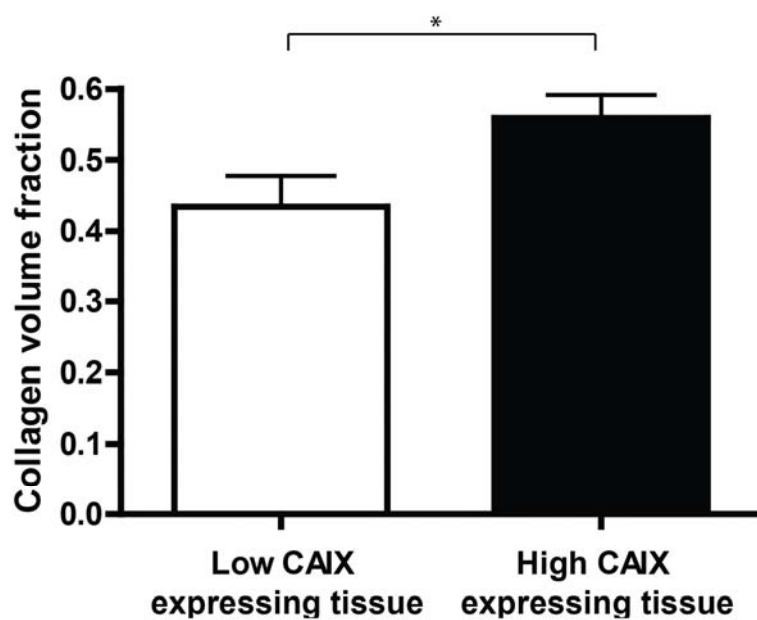
**E****MTC stained cardiac tissue****Digital mark-up image output from positive pixel algorithm**



**F****Grade 0 - Normal****Grade 1 - Minimal Fibrosis****Grade 2 - Mild Fibrosis****Grade 3 - Moderate Fibrosis****Grade 4 - Severe Fibrosis****Grade 5 - Extensive Fibrosis**

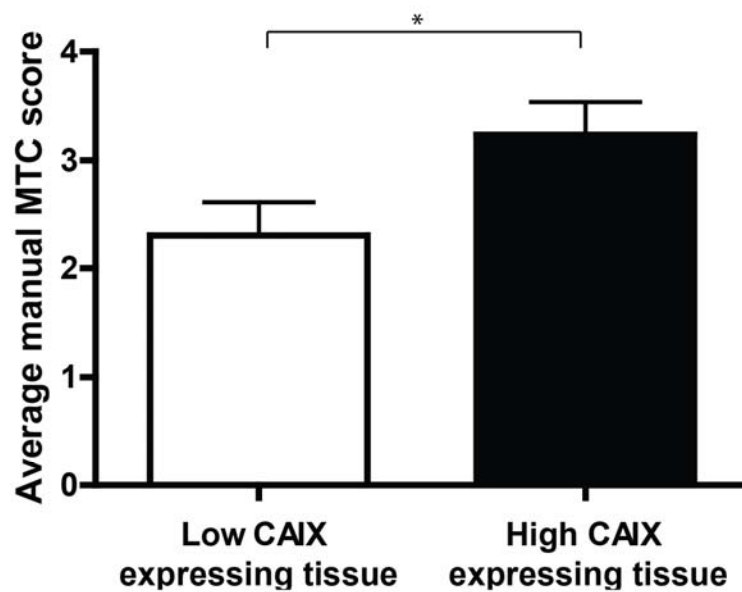
**G**

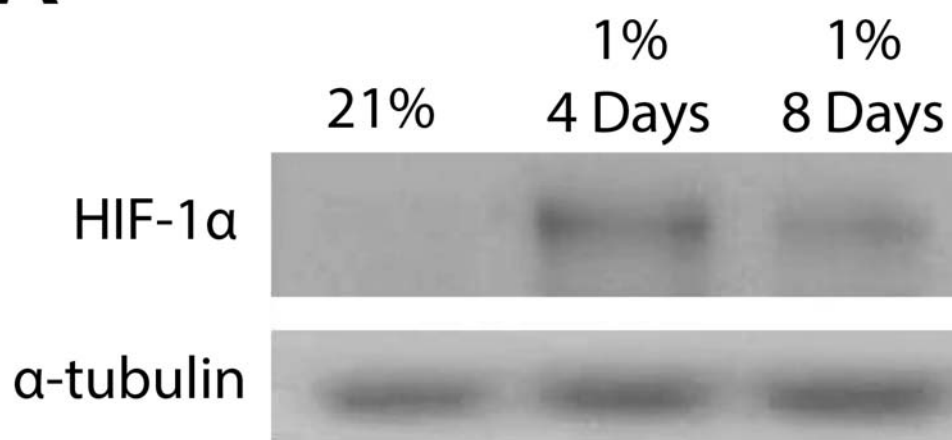
**Collagen deposition in relation to hypoxia  
as quantified by a positive pixel algorithm**

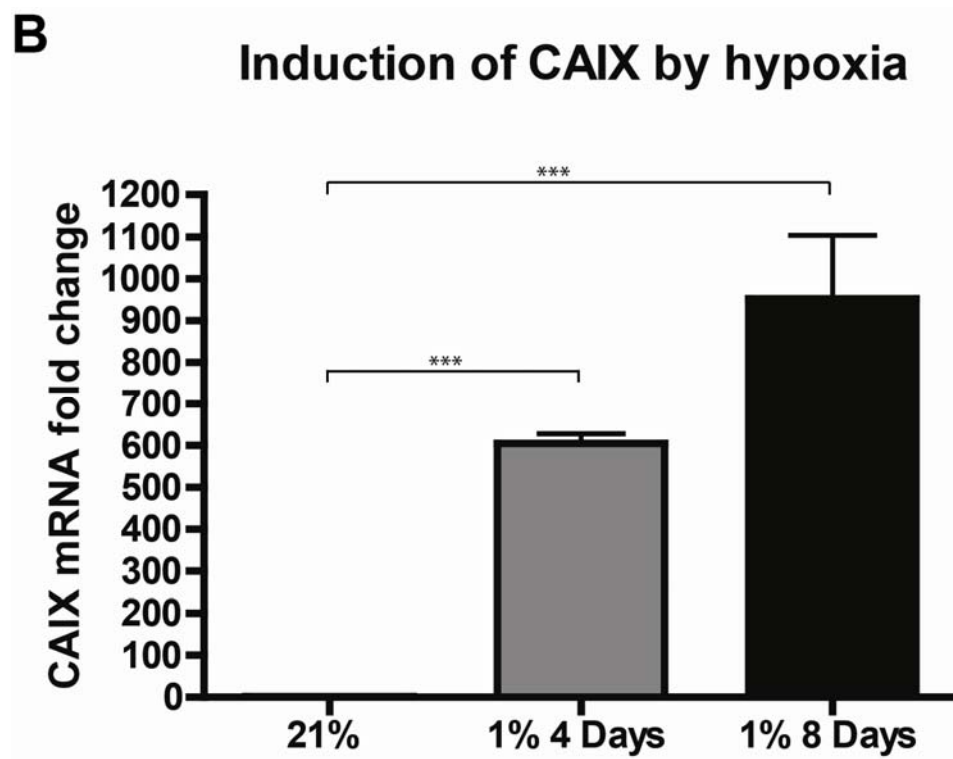


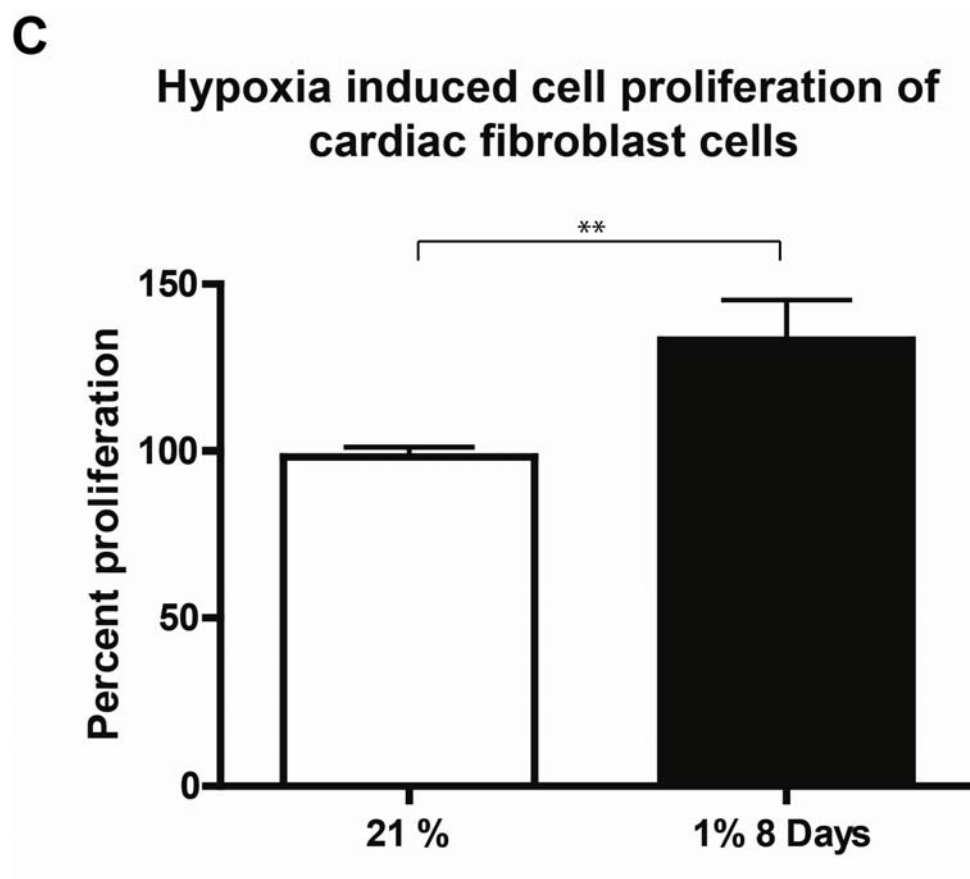
**H**

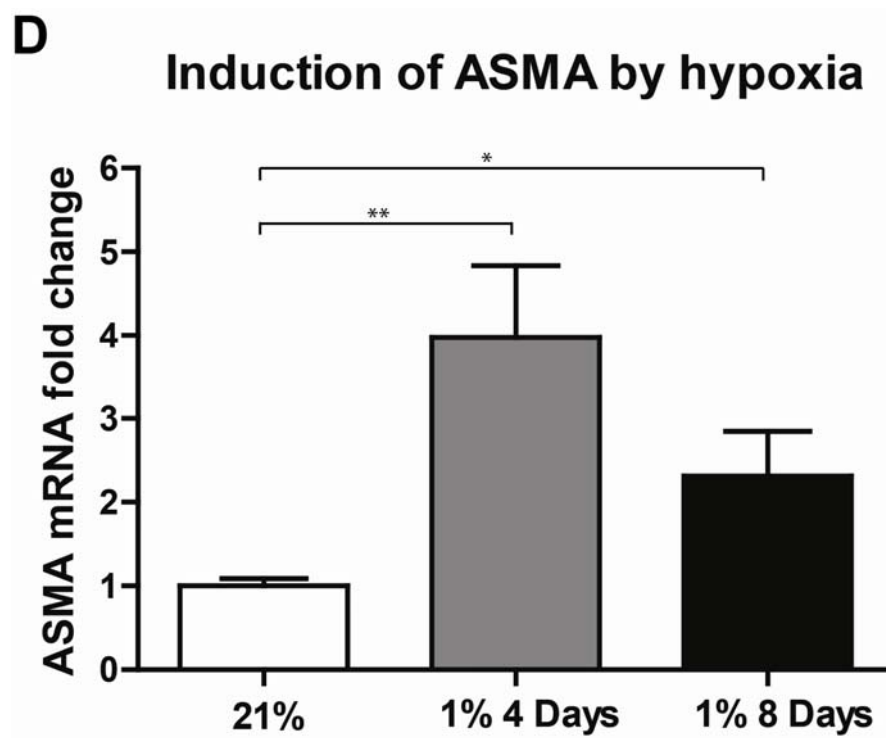
**Collagen deposition in relation to hypoxia  
as quantified by manual scoring**

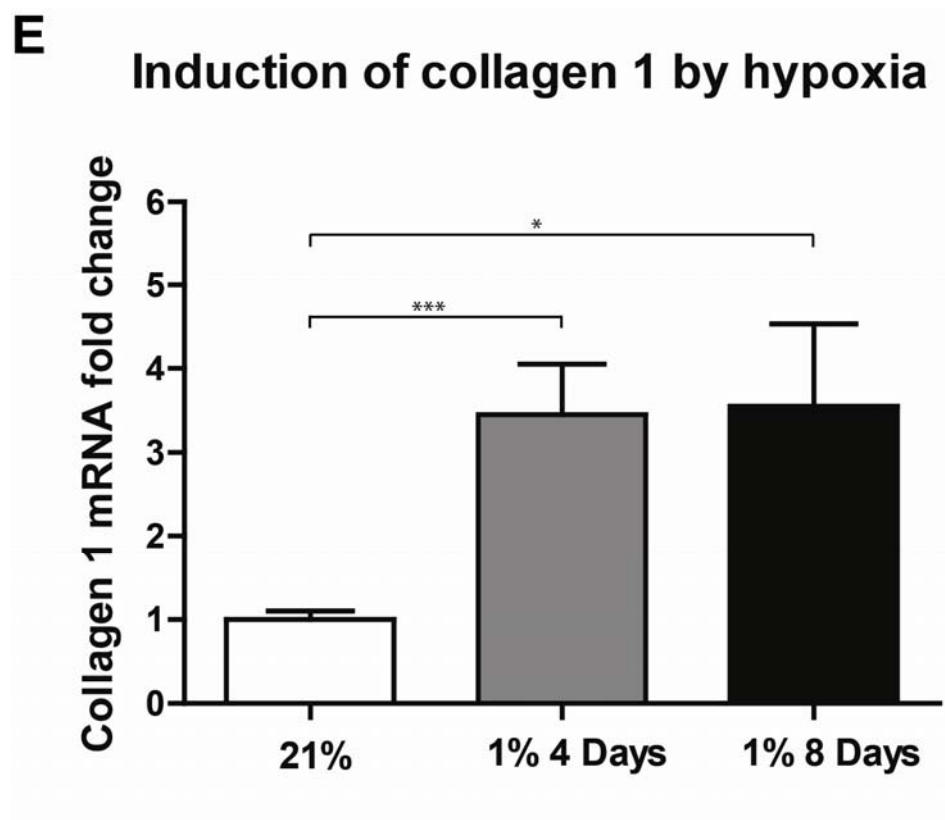


**A**

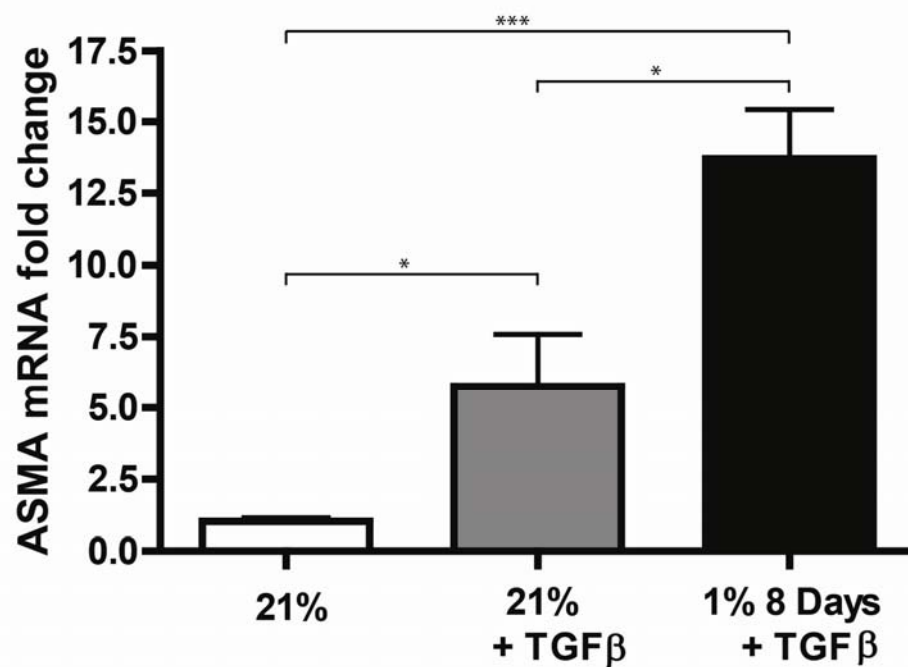






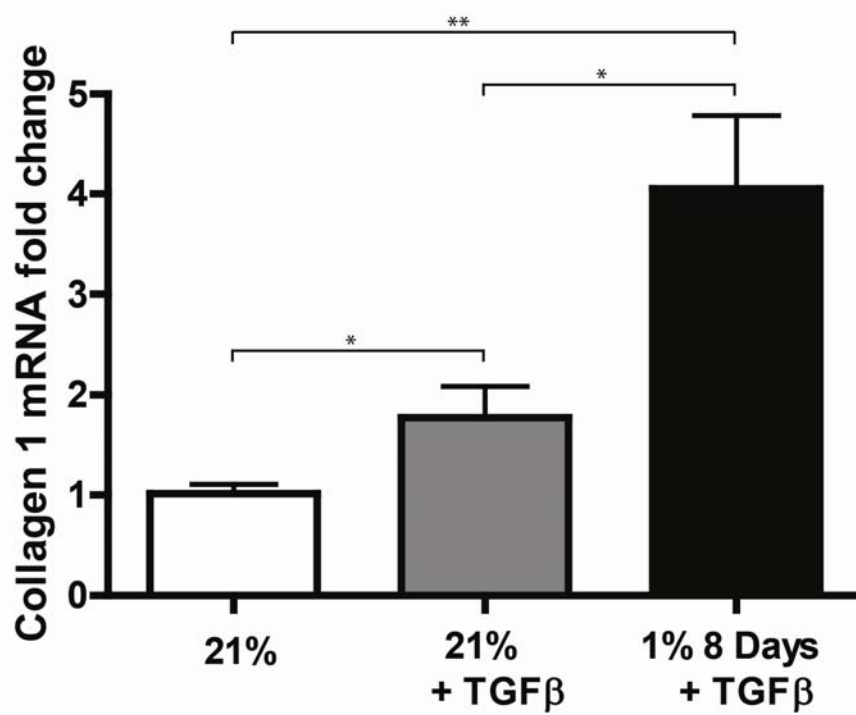




**F****TGF $\beta$  induction of ASMA in hypoxia**

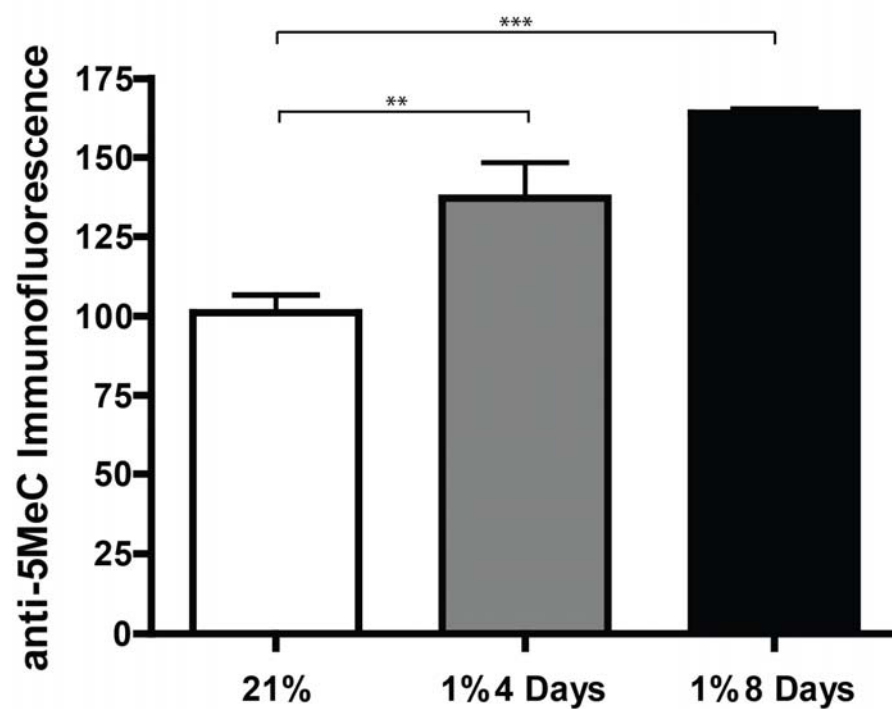
# G

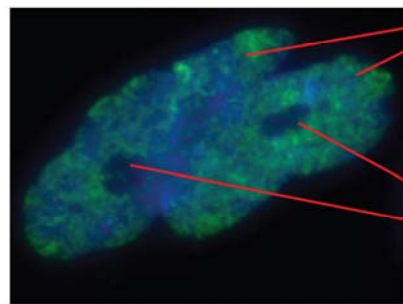
## TGF $\beta$ induction of collagen 1 in hypoxia



# A

## Hypoxia induces global DNA hypermethylation



**B**

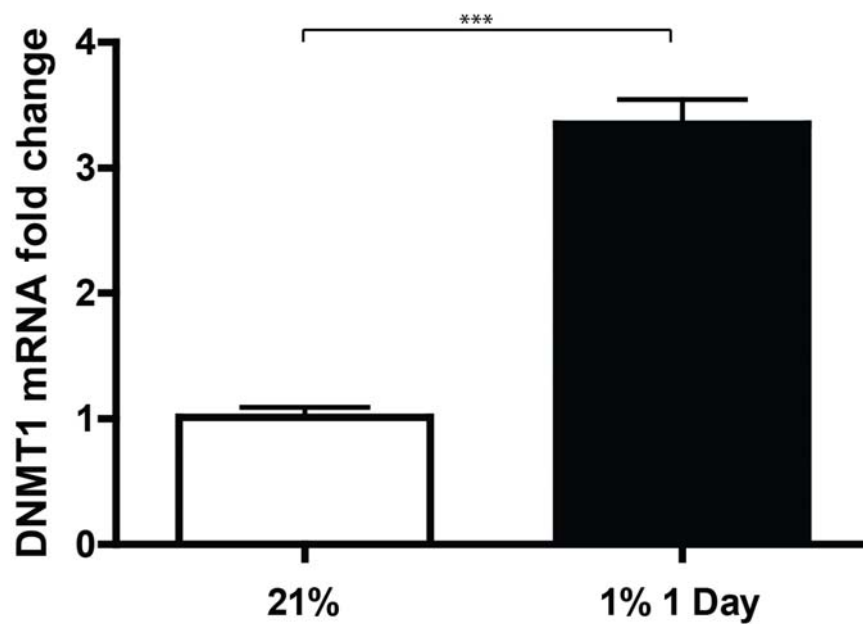
2 elongated fibroblast nuclei

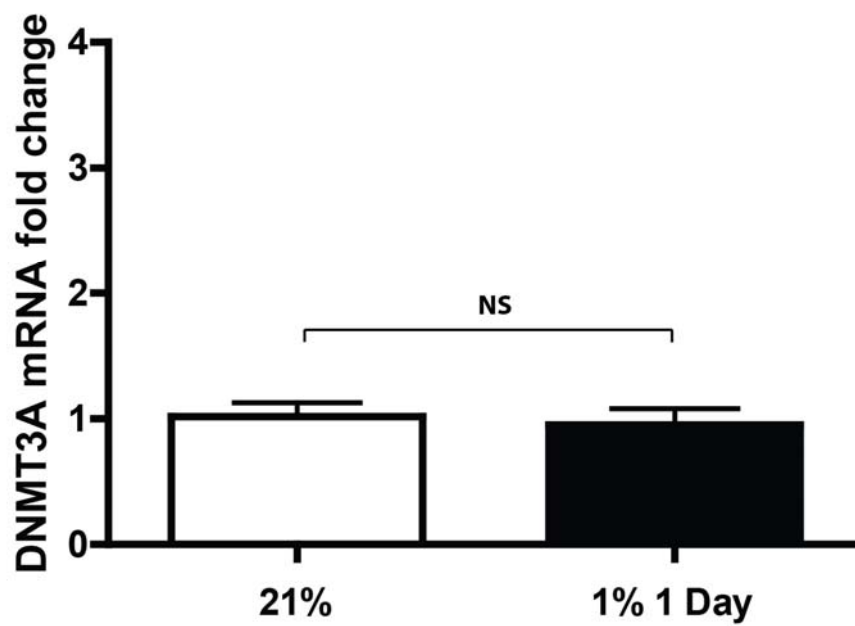
- green: anti-5-MeC/FITC

- blue: DAPI nuclear counterstain

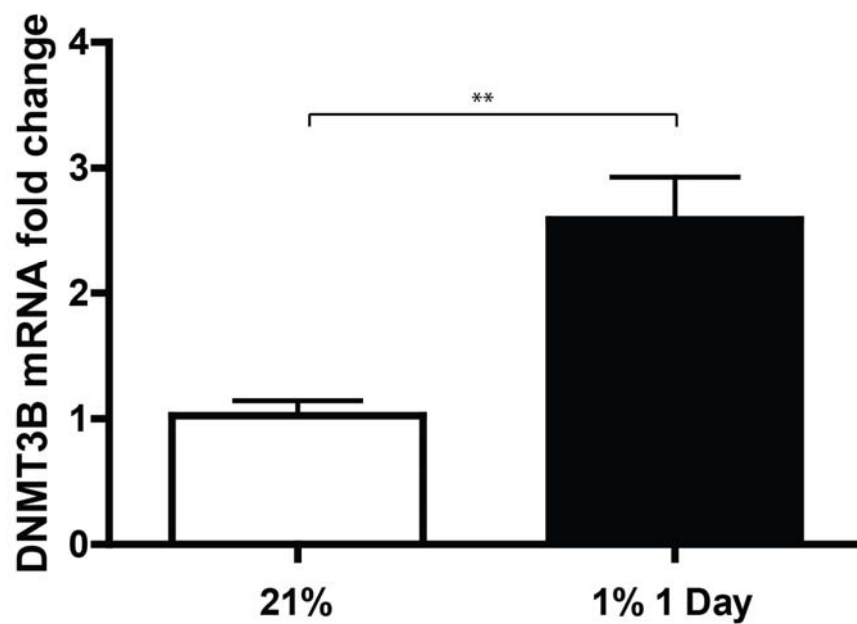
nucleoli

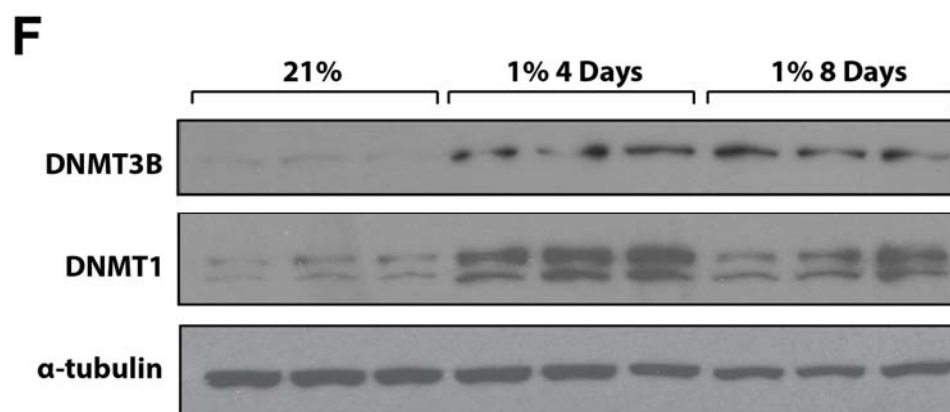
### C Induction of DNMT 1 by hypoxia



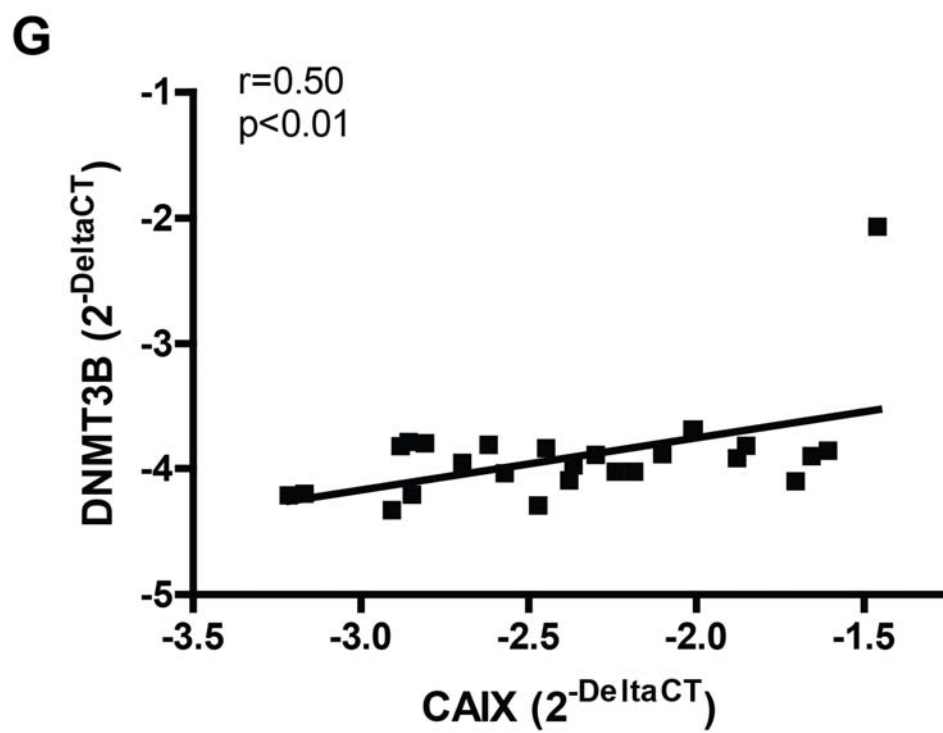
**D****Induction of DNMT 3A by hypoxia**

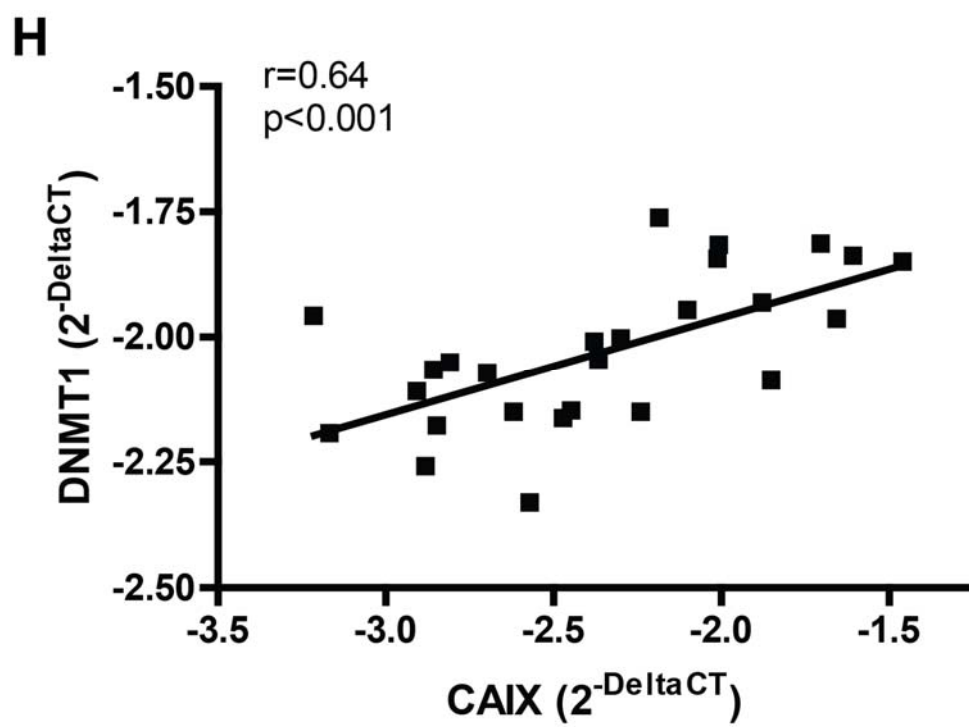
# **E** Induction of DNMT 3B by hypoxia

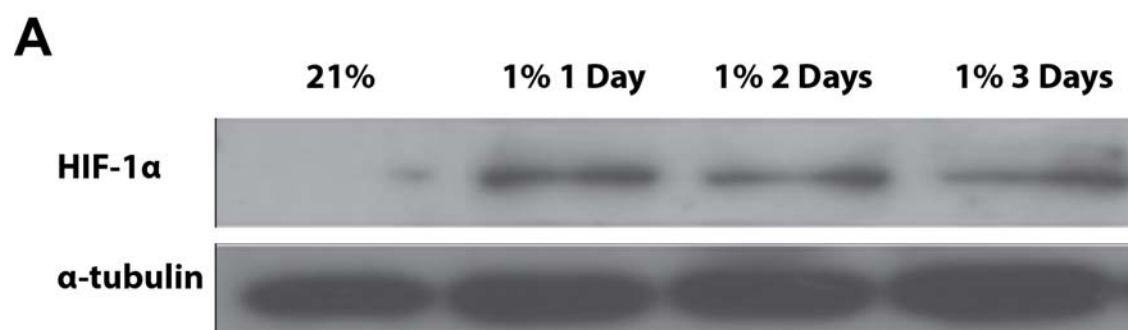


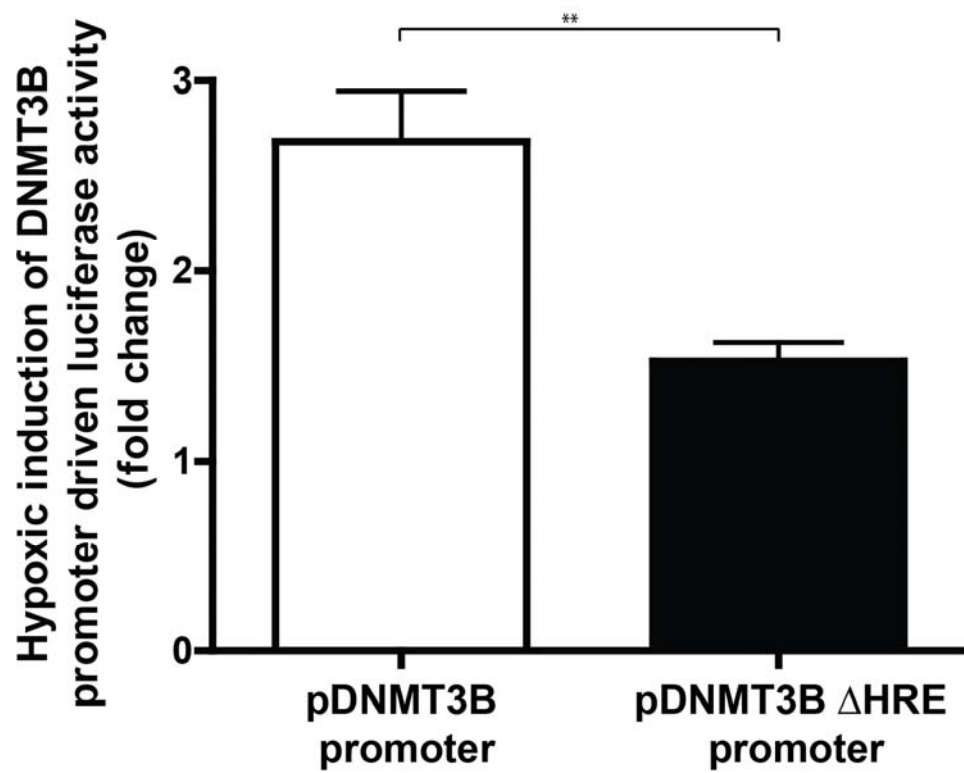


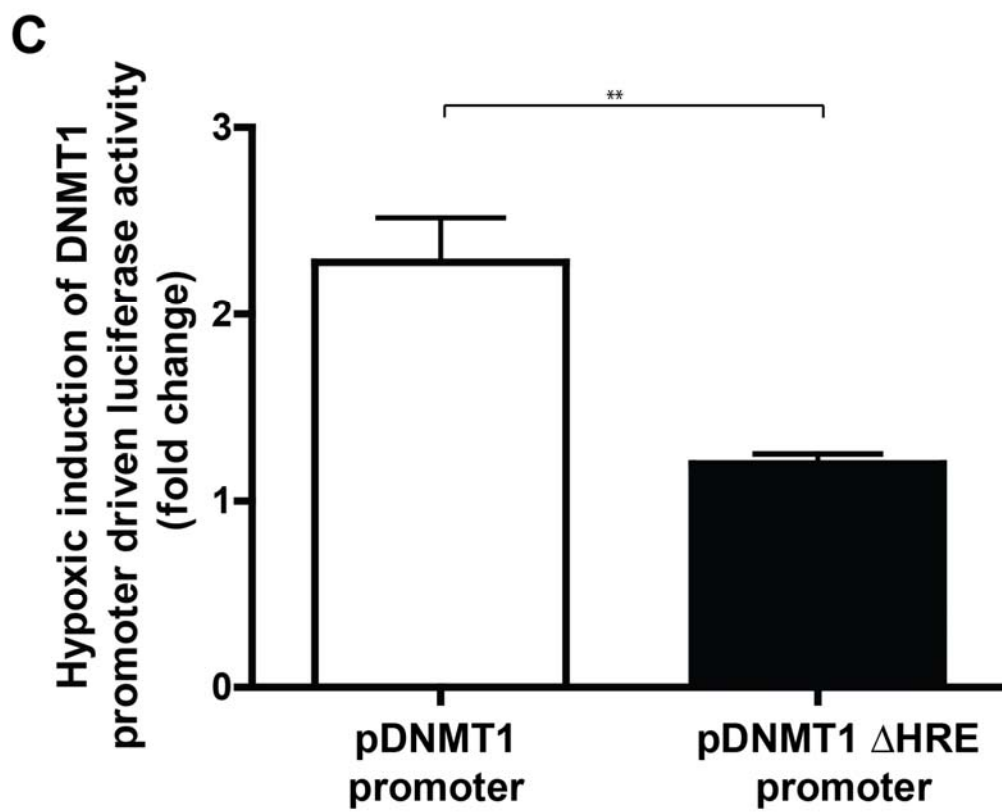


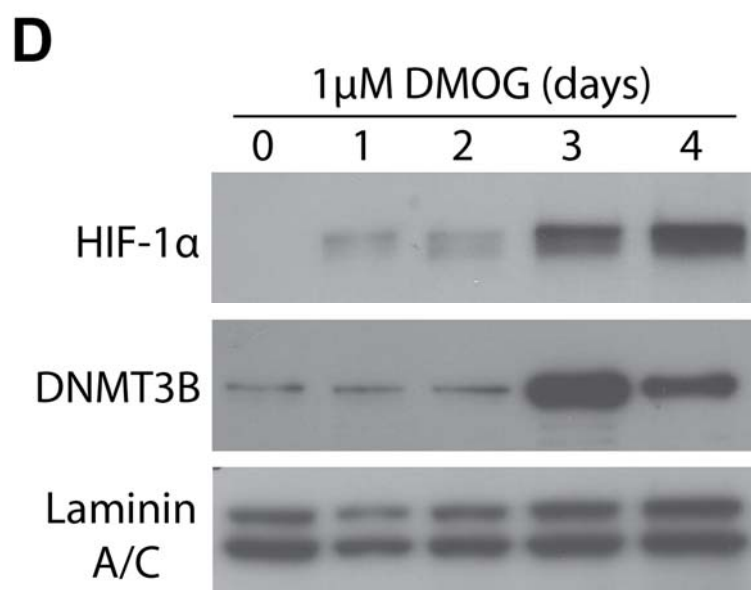


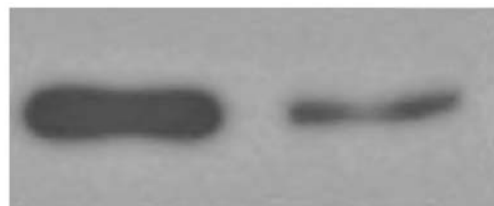
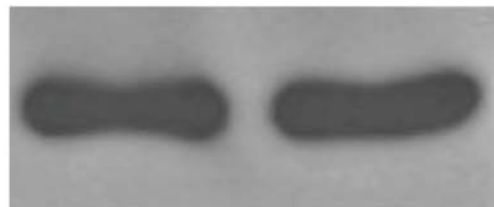


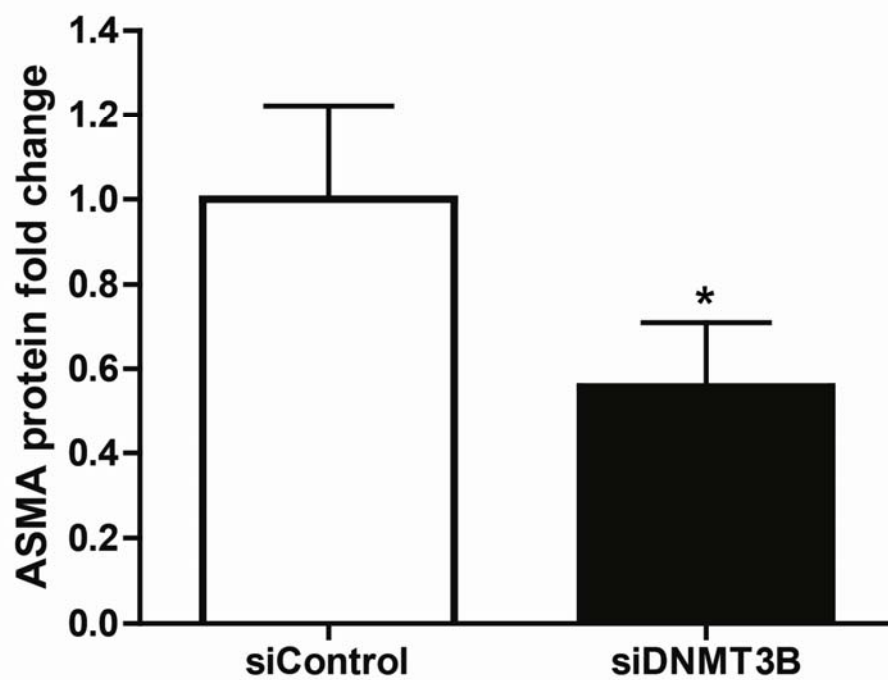


**B**

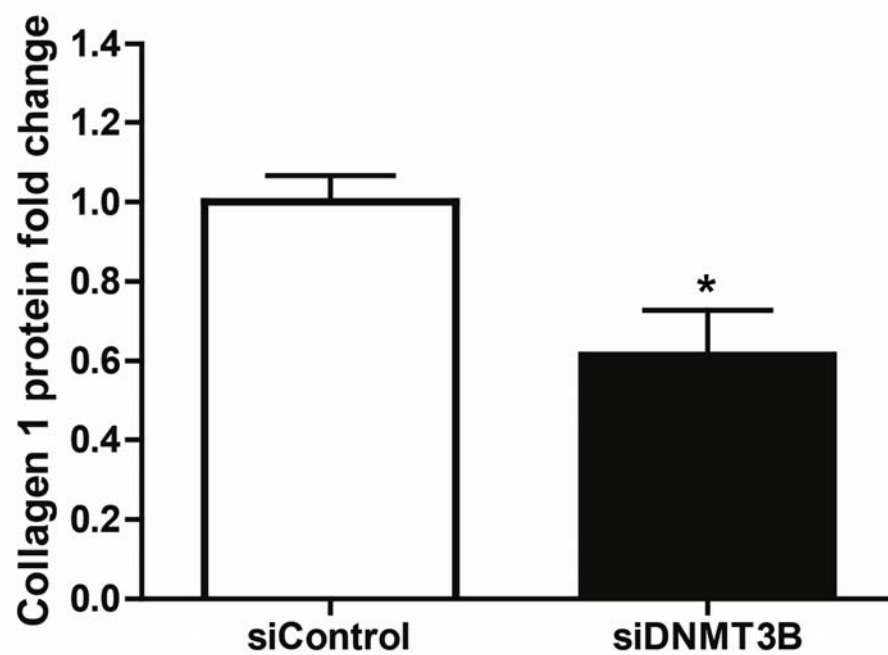




**A****siControl siDNMT3b****Collagen 1****ASMA****DNMT3B** **$\alpha$ -Tubulin**

**B****Supression of ASMA by siDNMT3B**



**C****Supression of collagen 1 by siDNMT3B**

**D****TGF induction of ASMA in hypoxia is inhibited by 5-aza**